BENCH SCALE LEACHING STUDIES ON URANIUM MILL TAILINGS

By

SURESH KUMAR YAGNIK, B. Tech.

A Thesis

Submitted to the School of Graduate Studies

in Partial Fulfilment of the Requirements

for the Degree

Master of Engineering

McMaster University

Hamilton, Ontario, Canada

June, 1978

BENCH SCALE LEACHING STUDIES ON URANIUM MILL TAILINGS

MASTER OF ENGINEERING (1978) McMaster University
(Chemical Engineering) Hamilton, Ontario

TITLE: Bench Scale Leading Studies on Uranium Mill Tailings

AUTHOR: Suresh Kumar Yagnik, B. Tech. (Indian Institute of Technology, Kanpur, India)

SUPERVISORS: Dr. M.H.I. Baird and Dr. S. Banerjee

NO. OF PAGES: x, 102

ABSTRACT

Uranium-bearing ore is crushed and leached to extract uranium in an ore processing plant. However, the decay products of uranium are discarded as wastes or tailings from the plant. One such decay product is Ra^{226}, which is quite toxic and mobile. It remains dispersed with the tailings and spreads into air and potable waters from the tailing areas due to natural forces and decay to gaseous Rn^{222}.

In this work, bench scale leaching of the uranium mill tailings was done with a view to extract Ra^{226} into the liquid phase. A gamma counting technique for determination of Ra^{226} concentrations in solid and liquid samples was also developed. Details of sample preparation, ingrowth, and calibration are discussed. For extraction of radium, several extractants such as water and solutions of $CaCl_2$, EDTA, DTPA and HNO_3 were used. Effects of solid to liquid ratio and time of contact on the extraction of Ra^{226} were studied for these extractants. In some cases, effects of temperature, concentration of extractant and multiple cross current contacting were also studied. The results of various leaching experiments are interpreted.

The main results show that equilibrium distribution of radium between the extractants and tailings was attained rapidly. In all experiments, a fraction of radium was "unextractable", i.e., all operating lines had an intercept when extrapolated to zero solid to liquid ratio. In general, the operating lines had a relatively small slope indicating that high solid to liquid ratio could be used without significantly degrading extraction.

ACKNOWLEDGEMENTS

The work described in this thesis was co-supervised by Professor M.H.I. Baird of the Department of Chemical Engineering and Professor S. Banerjee of the Department of Engineering Physics. The author is grateful to his supervisors for their guidance, interest and cheerful encouragement throughout the work. The author is thankful to Professor J.E. Robinson for permitting the use of facilities in the Radiation Effects Laboratory.

Thanks are due to Process Development Department of Rio Algom Limited, Elliot Lake for providing two shipments of uranium mill tailings for use in this work. Discussions with John Jaipow of Ontario Department of Health, Jim Skeaff of CANMET, Ottawa, and Paul Wilkinson of C.C.I.W., Burlington in the early stages of this work were of great help.

Financial assistance from McMaster University is also thankfully acknowledged.

TABLE OF CONTENTS

LIST OF TABLES

LIST OF FIGURES

CHAPTER 1

BACKGROUND INFORMATION

1.1 INTRODUCTION

Uranium is, at present, the only commercial fuel material for nuclear power reactors. With decreasing availability of oil and gas, the uranium industry is of great significance in meeting future energy needs. In Canada, the production of uranium was equivalent to 6300 and 7500 short tons U_3O_8 in 1976 and 1977, respectively (1). Most of this uranium comes from mines and ore processing plants near Elliot Lake and Bancroft in Ontario. In Northern Saskatchewan, there are uranium mines and ore processing plants near Uranium City and Rabbit Lake. The importance of the uranium industry in Canada is evidenced by the fact that exploration activity of one kind or other is in progress in virtually every province.

Production of nuclear grade uranium from its ores involves several steps. The uranium bearing ore contains decay products which come from the uranium isotope decay chains. When the ore is crushed and leached to extract uranium, most of the decay products remain in the residue, called mill tailings.

Some of the decay products are long-lived radioisotopes. The mill tailings, therefore, contain radioactive materials and may require special treatment to protect the surrounding environment. Ra^{226}, an isotope of radium, is one such decay product which is quite mobile. It can spread into air and water from the mill tailings. Although there are several

methods of controlling the spread of Ra^{226}, none of them appear to offer a long-term solution.

It would be desirable to remove the long-lived decay products (in particular, Ra^{226} and Th^{230}) from the residue in the form of concentrates that can then be treated in the same way as high level wastes from nuclear reactors. The motivation for this study was to look for methods which could remove a large fraction of mobile radium from the mill tailings.

The uranium decay chains, uranium ore processing, and radioactive nature of mill wastes, are briefly described in the rest of this chapter. In the next chapter, the objectives of this work will be clearly defined.

1.2 URANIUM AND ITS DECAY CHAINS

Uranium is so widely spread that it is sometimes called a ubiquitous element. The abundance of uranium is far better known than that of other elements because of its radioactivity. Using sensitive detectors of radioactivity, it is possible to detect very low concentrations of uranium. Uranium is generally found in igneous and sedimentary rocks, ocean and river waters, and even in living matter (2). At present, more than 150 uranium minerals are known (3).

Naturally occurring uranium is made up of three isotopes, namely U^{238}, U^{235} and U^{234}. U^{238} and U^{235} occur to the extent of 99.3% and 0.7%, respectively, whereas the third isotope, U^{234}, is present in trace quantity (about 5×10^{-6}%). U^{238}, having the longest half-life among these isotopes, eventually decays to Pb^{206} which is stable. The transformation of U^{238} into Pb^{206} is not a one-step process. The decay occurs through

a series of radioisotopes, each having a different half-life. The decay chain is called the Uranium Series. U^{234} is a member of the Uranium Series. However, U^{235} is the first member of an independent decay chain called the Actinium Series which ends with stable Pb^{207}.

Uranium deposits are usually found with Th^{232}, the main isotope of thorium. Th^{232} is another naturally occurring radioisotope having yet another decay chain of its own which ends with stable Pb^{208}. This series is called the Thorium Series.

The three decay chains described above are given in Tables 1.1-1.3 with the half-lives of each radioisotope and the type of radioactive emission and its energy. These decay chains will be later referred to in Chapter 3, where a gamma counting technique for determination of Ra^{226} concentration is described.

When the rate of disintegration of every member of a decay chain attains the same value, the series is said to have reached secular equiligrium. Most uranium ores have remained undisturbed long enough that it is reasonable to assume a state of secular equilibrium (5),(6) for the U^{238} series. In such a state, the amount of each daughter product is proportional to the half-life.

1.3 PRODUCTION OF URANIUM CONCENTRATE(2),(3),(7),(8)

Exploration, mining and subsequent recovery of uranium are basic steps in a nuclear fuel cycle. Uranium is mined by the open-pit or underground methods, depending on the depth at which the ore is available. Large deposits near the surface are mined by the open-pit method. At greater depths, waste-to-ore ratio becomes very large and underground

Table 1.1 Uranium Series (4n + 2)

Nuclide	Half-life	Energy, MeV, (1MeV = 1.602×10^{-13} J) Alpha[a]	Beta	Gamma (photons dis.)[b]
$^{238}_{92}U$	4.51×10^{9} y	4.18		
$^{234}_{90}Th(UX_1)$	24.10 d		0.193,0.103	0.092(0.04),0.063(0.03)
$^{234m}_{91}Pa(UX_2)$	1.175 m		2.31	1.0(0.015) 0.76(0.0063),I.T.
$^{234g}_{91}Pa(UZ)$	6.66 h		0.5	Many weak
$^{234}_{92}U(UII)$	2.48×10^{5} y	4.763		
$^{230}_{90}Th(I_0)$	8.0×10^{4} y	4.685		0.068(0.0059)
$^{226}_{88}Ra$	1,622 y	4.777		
$^{222}_{86}Rn$	3.825 d	5.486		0.51 (very weak)
$^{218}_{84}Po(RaA)$	3.05 m	5.998 (99.978%)[c]	Energy not known(0.022%)[c]	0.186(0.030)
$^{218}_{85}At(RaA')$	2 s	6.63 (99.9%)[c]	Energy not known (0.1%)[c]	
$^{218}_{86}Rn(RaA")$	0.019 s	7.127		
$^{214}_{82}Pb(RaB)$	26.8 m		0.65	0.352(0.036),0.295(0.020 0.242(0.07)
$^{214}_{83}Bi(RaC)$	19.7 m	5.505 (0.04%)[c]	1.65,3.7 (99.96%)[c]	0.609(0.295),1.12(0.131)
$^{214}_{84}Po(RaC')$	1.64×10^{-4} s	7.680		
$^{210}_{81}Tl(RaC")$	1.32 m		1.96	2.36(1),0.783(1),0.297(1
$^{210}_{82}Pb(RaD)$	19.4 y		0.017	0.0467(0.045)
$^{210}_{83}Bi(RaE)$	5.00 d		1.17	
$^{210}_{84}Po(RaF)$	138.40 d	5.298		0.802(0.000012)
$^{206}_{82}Pb(RaG)$	Stable			

(a),(b),(c) See Footnotes under Table 1.3.

Ref. (4).

Table 1.2 Actinium Series (4n + 1)

Nuclide	Half-life	Energy, MeV Alpha[a]	Beta	Gamma (photons dis.)[b]
$^{235}_{92}U$	7.13×10^8 y	4.39		0.18(0.7)
$^{231}_{90}Th$(UY)	25.64 h		0.094,0.302, 0.216	0.022(0.7),0.0085(0.4) 0.061(0.16)
$^{231}_{91}Pa$	3.43×10^4 y	5.049		0.33(0.05),0.027(0.05) 0.012(0.01)
$^{227}_{89}Ac$	21.8 y	4.94(1.2%)[c]	0.0455 (98.8%)[c]	
$^{227}_{90}Th$(RdAc)	18.4 d	6.03		0.24(0.2),0.05(0.15)
$^{223}_{87}Fr$(AcK)	21 m		1.15	0.05(0.40),0.08(0.24)
$^{223}_{83}Ra$(AcX)	11.68 d	5.750		0.270(0.10),0.155(0.055)
$^{219}_{86}Em$(An)	3.92 s	6.824		0.267(0.086),0.392(0.048
$^{215}_{84}Pa$(AcA)	1.83×10^{-3} s	7.635		
$^{211}_{82}Pb$(AcB)	36.1 m		1.14,0.5	Complex spectrum, 0.065 to 0.829 MeV
$^{211}_{83}Bi$(AcC)	2.16 m	6.619 (99.68%)[c]	Energy not known(0.32%)[c]	0.35(0.14)
$^{211}_{84}Po$(AcC')	0.52 s	7.434		0.88(0.005),0.56(0.005)
$^{207}_{81}Tl$(AcC")	4.78 m		1.47	0.87(0.005)
$^{207}_{82}PB$	Stable			

(a),(b),(c) See Footnotes under Table 1.3.

Ref. (4)

Table 1.3 Thorium Series (4n)

Nuclide	Half-life	Energy, MeV		
		Alpha[a]	Beta	Gamma (photons dis.)[b]
$^{232}_{90}Th$	1.39×10^{10} y	3.98		
$^{228}_{88}Ra$(MsTh1)	6.7 y		0.01	
$^{228}_{89}Ac$(MsTh2)	6.13 h		Complex decay scheme. Most intense Beta group is 1.11 MeV	1.59(n.v.) 0.966(0.2) 0.908(0.25)
$^{228}_{90}Th$(RdTh)	1.91 y	5.421		0.084(0.016)
$^{224}_{88}Ra$(ThX)	3.64 d	5.681		0.241(0.038)
$^{220}_{86}Em$(Tn)	52 s	6.278		0.542(0.0002)
$^{216}_{84}Po$(ThA)	0.158 s	6.774		
$^{212}_{82}Pb$(ThB)	10.64 h		0.35,0.59	0.239(0.40)
$^{212}_{83}Bi$(ThC)	60.5 m	6.086 (33.7%)[c]	2.25(66.3%)[c]	0.04 (0.034 branch)
$^{212}_{84}Po$(ThC')	3.04×10^{-7} s	8.776		
$^{208}_{81}Tl$(ThC")	3.1 m		1.80,1.29,1.52	2.615(0.997)
$^{208}_{82}Pb$(ThD)	Stable			

(a) Only the highest energy alpha is given.

(b) Only the most prominent gamma photons are listed.

(c) Indicates branching. The percentage enclosed in the parentheses gives the proportional decay by the indicated mode.

Ref. (4).

mining is necessary.

Uranium content in ores is normally expressed as the percentage of U_3O_8. A typical ore contains about 0.2% U_3O_8. In the processes following mining, uranium is extracted to produce uranium concentrate (yellow cake), containing more than 50% U_3O_8. This concentrate is then used to produce uranium of higher purity.

The ore processing plants producing uranium concentrate are usually located near the mines. Selection of the extraction process depends on several considerations such as chemical composition of minerals, degree of extraction desired and physical state of the ore. Due to these considerations, the processes used in different plants differ to some extent. Also, improvements in the extraction process are continually being done. However, there are the following essential features of the extraction process at present:

(1) sorting and crushing of the raw ore from mines;

(2) leaching the crushed ore with dilute acid or alkali;

(3) concentration of uranium from liquor obtained as a result of leaching by solvent extraction or ion exchange; and,

(4) precipitation of uranium from the resultant liquor.

Often, the liquor obtained from leaching (step 2 above) is reasonably free of impurities and further purification by solvent extraction or ion exchange is not necessary. In such a case, step 4 is performed directly on the liquor obtained from leaching. In the leaching process, about 90% Uranium is extracted from the ore discarding most of the decay products and impurities in the sand-like gangue which is called mill tailings in this work.

Sulfuric acid is most widely used in the acid leaching process. Acid leaching is done in rubber lined cylindrical or conical vessels with mechanical or pneumatic agitation. An oxidant is added in the leaching vessel to ensure all uranium in hexavalent (soluble) state. Increasing the acid temperature improves the extraction of uranium. The pH is maintained at 1.8 to minimize acid consumption.

For an alkaline leaching process, both sodium carbonate and sodium bicarbonate solutions are used. Leaching is done in mild steel vessels, mechanical stirring or air agitation is used as with acid leaching. The addition of bicarbonate prevents precipitation of uranium owing to excessive alkalinity. An oxidant is used in this case also to oxidize uranium to the hexavalent state.

Alkaline leaching has advantages over acid leaching as it is non-corrosive and tends to attack only uranium minerals leaving most of the impurities of the gangue unattacked. However, some uranium minerals fail to dissolve in the alkali. Thus, the alkaline process cannot be used for all types of uranium ores.

Fig. 1 shows the flowsheet for production of uranium concentrate from Canadian pitchblende ore. This process selectively removes impurities from the liquor obtained from acid leaching of the crushed ore. Ion exchange or solvent extraction is not used. The ore from the mines is first crushed in ball mills and magnetite is separated in a magnetic separator. Light gangue is then separated in flotation cells. The product of flotation cells is dried in furnaces at 600°C which decomposes sulfides, carbonates and volatalizes part of the arsenic and antimony. Sodium chloride is then added at 800°C to convert silver to

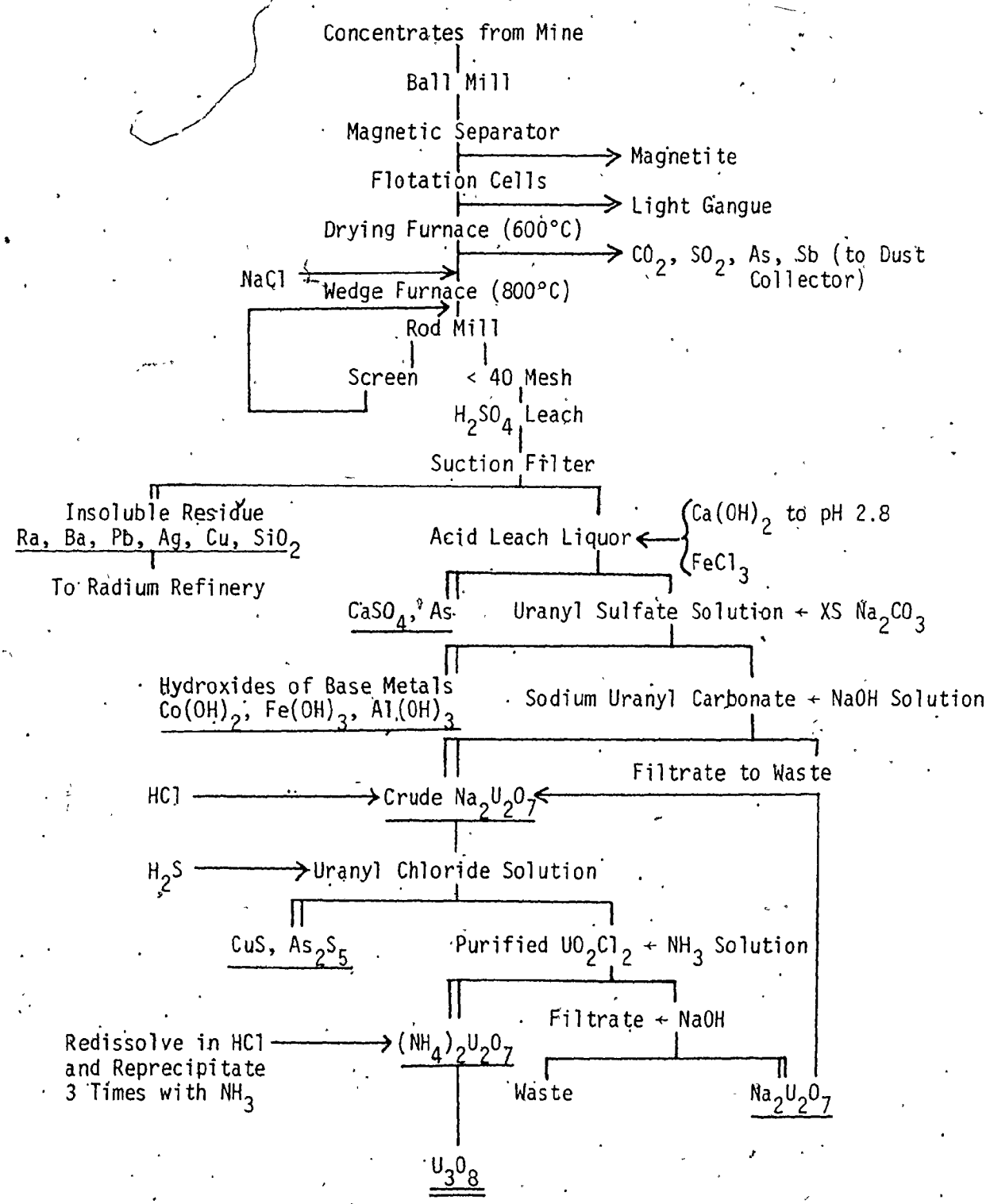

Figure 1: Flow Sheet for Production of U_3O_8 from Canadian Pitchblende at Port Hope (Ontario) Refinery

AgCl. After cooling, this material is leached with sulfuric acid to recover most of the uranium in the liquid. The insoluble residue (tailings) contain Ra, Ba, Pb, Ag, Cu and SiO_2. The acid leach liquor has several impurities along with the uranium. Part of the arsenic is removed from the liquor by addition of $Ca(OH)_2$ and $FeCl_3$ at pH 2.8. The arsenic is filtered as insoluble precipitate. To the filtrate, a sufficient quantity of Na_2CO_3 is added to solubilize uranium and separate cobalt, iron and aluminium as hydroxides. The remaining process involves addition of sodium hydroxide to the liquor so obtained to precipitate crude sodium diuranate ($Na_2U_2O_7$), which is then dissolved in hydrochloric acid. The solution is treated with H_2S gas which removes copper and remaining arsenic as sulfide precipitates. The filtrate is boiled to remove excess H_2S and then NH_3 is repeatedly added to recover uranium as $(NH_4)_2U_2O_7$. This is converted to U_3O_8 by ignition at 1000°C.

Leaching may dissolve large amounts of metals other than uranium from the ore. Some processes use ion exchange or solvent extraction to purify the pregnant leach liquor instead of a scheme of selective precipitation used in the process described above. The principle of ion exchange is that uranium forms anions in sulfate solution which exchange with anion-exchange resins. The uranium so adsorbed on the resins can be eluted by solutions of ammonium nitrate or sodium chloride. On the other hand, in solvent extraction uranium is selectively extracted from leach liquor in a suitable organic solvent. The solvents used are alkyl amines or alkyl phosphoric acid with diluents. The extraction is carried out in countercurrent mixer settlers. Uranium is then precipitated from the resultant liquor.

1.4 RADIOACTIVE WASTE FROM URANIUM MILLS

When uranium ore is leached in a mill, the state of secular equilibrium existing in the three decay chains described in section 1.2 is disturbed. This happens because of selective removal of uranium and the different leachability of each member in the leachant. Since primarily uranium is recovered by leaching, almost all decay products go with the tailings.

When secular equilibrium is disturbed, the short-lived daughter products decay quickly to negligible amounts. Only the long-lived decay products are a cause for concern in the mill waste (7),(9). Also, only decay products of U^{238} are important since U^{235} and Th^{232} occur in much lower concentrations in the original ore. Table 1.4 lists comparatively long-lived decay products in the Uranium Series.

Table 1.4 Long-Lived Decay Products in Uranium Series

Decay Product	Half-Life	Radiation
U^{234}	2.48×10^5 y	α
Th^{230}	8.0×10^4 y	α,γ
Ra^{226}	1622 y	α
Pb^{210} (RaD)	19.4 y	β,γ

Of the decay products listed in Table 1.4, Ra^{226} is the most hazardous. There will be further discussion on Ra^{226} and its biological effects in the following chapter.

In summary, this chapter has described the motivation of this work, uranium decay chains, uranium ore processing and the radioactive

nature of the wastes from the ore processing plants. This background information will be used in further discussions.

CHAPTER 2

THE RADIUM PROBLEM

Since the U_3O_8 content of a typical ore is only 0.2%, most of the ore fed into a uranium mill appears as waste or tailings. For every 1000 kg of ore (averaging 0.2% U_3O_8), approximately 600 uCi of Ra^{226} will appear in the tailings.* Thus, the tailings can be considered as enormous amounts of wastes in which small quantities of long-lived radioisotopes are dispersed. Ths discussion about the milling process in Chapter 1, also indicates that the waste stream from a uranium mill has wash water process chemicals and other impurities along with sand-like tailings.

2.1 OBJECTIVES OF THIS WORK

Due to its long half-life, toxicity and mobility, Ra^{226} in the tailings deserves the most attention. As discussed later in this chapter, most of the Ra^{226} in the ore remains with the solid tailings. It would be desirable to extract most of the radium into the liquid phase so that radium-containing liquid could be treated in some way (e.g., coprecipitation, ion-exchange) to obtain the radium in concentrated form. Such a high level radium waste, considerably reduced in mass could easily be disposed of by underground (geologic) disposal techniques.

---

* If one assumes secular equilibrium in the ore, Ra^{226} is 359 ppb in natural uranium. Also for Ra^{226}, 1g is equivalent to 1 Ci of activity.

Another suggested (10) possibility is to recover the radium from the tailings and incorporate it into reactor fuel.* The burn-up of Ra^{226} is feasible in a thermal neutron absorption step

$$Ra^{226} + \text{neutron} \rightarrow Ra^{227}$$
$$1622\ y \qquad\qquad 41.2\ m$$

has a cross-section of 20 barns for thermal neutrons. The radium then enters the actinide series through β decay of Ra^{227},

$$Ra^{227} \longrightarrow Ac^{227}$$
$$41.2\ m \xrightarrow{\beta^-} 22\ y$$

Thermal neutral absorption of actinides is generally easy and it is even possible to eventually obtain fissionable isotopes such as Th^{229} from original Ra^{226}.

Development of an extraction process for Ra^{226} would require a systematic study of the leachability of radium in various extractants. To do this, we obtained two shipments of dried solid tailings from the uranium mills at Elliot Lake. The objective was to carry out bench scale leaching studies with these tailing samples. To determine radium concentration, it was also necessary to develop a relatively simple and reliable analytical technique.

Based on these considerations, it was decided to concentrate on two main objectives:

(a) Working out a reasonably reliable and simple analytical technique for Ra^{226} and validating the technique;

---

* There are doubts about the feasibility of this suggestion because of the possible hazards in handling the fuel and difficulty in reprocessing spent fuel with Ra^{226} in it.

(b) Carrying out bench scale leading studies with some promising extractants and interpreting the results obtained.

2.2 RADIUM DISTRIBUTION IN URANIUM MILLING

Like several other decay products, almost all the radium present in the original ore appears in the mill tailings. According to a Winchester Laboratory study (11), approximately 93-97% radium in a sulfuric acid mill circuit and 97-98% radium in an alkaline mill circuit were found in the tailings. These percentages might vary a little from one mill to another. It is, however, well established that a very large fraction (12) of radium is discarded with the tailings. Large amounts of tailings are accumulated near virtually every uranium mill in the world (13) in "tailing piles" or "tailing ponds".

2.3 TOXICITY OF RADIUM

Some radiations produce ionizing effects in living tissues. Thus, both sudden exposure to high level radiations and chronic exposure to low level radiation may be harmful to human beings. It is, therefore, necessary to minimize environmental and occupational hazards associated with radioactive substances. There seems to be a threshold radiation dose which can be tolerated by a normally operating physiological mechanism without any medically perceivable effect. This threshold value of radiation dose is usually obtained from animal experimental data and clinical data. The Maximum Permissible Concentrations (MPC) of the radioactive substance in air and water are recommended by reducing the threshold dose by an appropriate safety factor (4). Several other considerations such as type of the radionuclide, critical organ, biological half-life, etc. are also considered in calculation of MPC. If the radiation exposure is caused by more than one radionuclide present in different concentrations, then,

$$\frac{C_1}{(MPC)_1} + \frac{C_2}{(MPC)_2} + \ldots + \frac{C_n}{(MPC)_n} \leq 1$$

should be satisfied. Here $C_1, C_2, \ldots, C_n$ and $(MPC)_1, (MPC)_2, \ldots, (MPC)_n$ are concentrations and maximum permissible concentrations of different radionuclides.

Ra^{226} is classified as a "very highly toxic" radionuclide by health physicists. It emits 4.77 MeV alpha particles and is indirectly responsible for several alpha, beta and gamma emitting progeny (c.f. Table 1.1). Alpha radiations are particularly harmful if emitted inside a living body because of their short ranges (and therefore more severe ionizing effects per unit volume). The maximum amount of radium that may be tolerated when fixed in the body for a long time is 0.1 μCi (14). If radium is ingested, elimination is very rapid for the first few days. However, the rate of elimination decreases with time. Most of the retained radium deposits in the bones and may cause bone cancer (15).

Ra^{226} is the precursor of Radon (Rn^{222}) in Uranium Series. Gaseous Rn^{222} could diffuse out of a tailing particle having Ra^{226} in it. The percentage of Rn^{222} which escapes from a particle is called the "emanating factor" which roughly ranges between 20-25% (16). Thus, tailing piles and tailing ponds continuously emanate radon. The half-life of Rn^{222} is relatively short (3.8 days) and it decays to several short-lived decay products which remain in the mine and mill environment in the form of fine airborne particles (16). In air, concentrations of Rn^{222} as low as 10^{-8} μCi/cm^3 will cause maximum permissible dose to lungs if breathed for a long time (14).

Natural forces such as wind, rain and snow also help to spread radium from tailing areas. The form in which radium is present in the

tailings is not clearly understood. For a sulfuric acid leached ore, radium may be present in the tailings in some complex or adsorbed form of $RaSO_4$. The solubility of pure $RaSO_4$ in water is 2.0×10^{-6} g/ml at 25°C (11) which is approximately equivalent to 1400 μCi Ra^{226}/litre. This value of solubility is rather low but it far exceeds the MPC_w of Ra^{226} in drinking water which is 3.0 pCi/l. Thus water draining and overflowing from tailing areas which eventually finds it way in nearby lakes or rivers may have several tens of picocuries of Ra^{226} per litre (13).

The foregoing discussion suggests that Ra^{226} in the tailing areas calls for relative isolation from the general public. Also, due to its mobility, Ra^{226} may contaminate the environment. For example, in the Animas River (downstream from a licensed uranium mill at Durango, Colorado) damage to fauna attributable to radium could be traced 50 miles downstream in 1958 (10). Prior to 1966, uranium tailings were used as a fill material for construction purposes. There are more than 5000 such buildings in the United States. The radon concentrations and gamma radiations in these buildings are causing considerable radiation exposure to the public. At present, not more than 20 pCi/g Ra^{226} is considered safe in soil and building materials (10).

A brief summary of current methods of controlling Ra^{226} from tailings to prevent environmental hazards are discussed in the next section.

2.4 CURRENT METHODS OF RADIUM CONTROL

There are three possible ways to approach the radium problem:

(a) The original ore may be treated to remove radium prior to recovery of uranium;

(b) The uranium recovery process could be modified in order to reduce the radium level in the tailings; and,

(c) Efforts can be made to control radium in the tailings from the conventional process.

At present, choice (c) is selected. Mill tailings (solid and liquid effluents) are treated in several ways to control radium. Choices (a) and (b) are not selected because the prime objective of the process is uranium extraction and not removal of radium. Further, choice (a) may cause possible loss of uranium in pretreating the ore to remove radium.

Each of the following methods to remove or control radium has been used and investigated with varying degrees of success.

2.4.1 Preventive Measures: To reduce hazards due to radium in the milling process, some recommended rules and regulations are followed in practice. These include (11),(16) the use of dust-tight equipment, proper ventilation, regular clean-up of premises and health check-up programs for personnel. Care should be taken to restrict the tailings areas from the public and to avoid discharges into potable waters.

2.4.2 Stabilization: This practice is used for inactive tailing areas (where no further tailings are being dumped). Stabilization consists of surface treatment of tailing piles and establishment of healthy grass cover on the tailing piles. This reduces environmental impact through prevention of dusting, considerable reduction in radon emanation and reduction of surface gamma radiation to acceptable levels (17).

Rubber and polymer sealants have also been used for the purpose of stabilizing the tailings piles (18).

2.4.3 Underground Disposal: This practice is very expensive in view of the large amounts of the tailings. Once the disposal well is constructed, routine injection of the wastes could be started. A mill near Grants, New Mexico uses this method sometimes.

2.4.4 Sand/Slime Separation: Most of the radium in the tailings appear in fine particles (17),(19), or slimes. Slimes do not settle readily in tailing ponds, therefore their separation from coarser particles could provide radium in concentrated form for separate storage or further treatment.

Sand/slime separation can be done by sedimentation. Flotation has been found (17) to be less effective. In this method, the coarser particles with acceptable levels of radium can be conveniently discharged and the slimes kept in restricted areas. If further treatment of slimes is necessary, this method would certainly reduce the cost of such a treatment since a smaller amount would have to be handled.

2.4.5 Barium Chloride Treatment: Liquid effluents containing radium at greater than acceptable levels can be treated by $BaCl_2$. To accomplish this, the pH of the effluent is raised to about 8 and $BaCl_2$ solution is added (50 to 300 mg $BaCl_2$ per litre of effluent). A low concentration ($\sim$ 0.01 M) of sulphate as sodium or ammonium makes the process more effective (20). The liquid need not be completely separated from the solids. In practice, $BaCl_2$ solution is added in tailing ponds (9) where solids are slowly settling. Addition of $BaCl_2$ coprecipitates $Ba(Ra)SO_4$, which also settles with the solids in the pond. Thus, the liquid overflowing the tailing ponds is essentially free of radium.

2.4.6 Ion Exchange: Neutralized liquid effluents from the uranium mill are treated with barytes and natural and synthetic zeolites (20),(21), to remove radium. Arnold and Crouse (21) performed packed column tests with zeolites and found that it is possible to reduce radium concentration to acceptable levels by this method.

None of the methods described in the foregoing sections gives a permanent solution to the radium problem. The last two methods, namely Barium Chloride Treatment and Ion Exchange are mainly for the liquid effluents which contain only a small percentage of total radium in the tailings. It is the solids which have considerable radium content and need attention for the control or removal of radium.

CHAPTER 3

MEASUREMENT OF RADIUM CONCENTRATION

This chapter is devoted to the first objective of this work, i.e., development of a suitable analytical technique (c.f. Section 2.1). There are several methods for determination of radium concentration. However, not all of them are simple and straightforward. For reasons to be discussed in this chapter, gamma counting with Ge(Li) detector was used for this work. The basic principles of gamma counting equipment, statistical considerations and calibration of the counting set-up are also discussed. Details regarding the experimental aspects of leaching studies and preparation of standard samples are also given.

3.1 ANALYTICAL TECHNIQUE

Radioactivity measurements are most frequently used for determination of radium. They are relatively simple and radium concentration can be determined with reasonable accuracy. However, gravimetric methods (22), emission spectrometry (23), photographic emulsions (24) and calorimetric methods (25) have also been used for determination of radium.

Radium analysis in tailing samples and liquid samples can be made by either alpha or gamma counting of radium and its daughters. Alpha counting of Radon was used by Rushing (26) to determine Ra^{226} in various samples. This method, called the Radon De-emanation Method, is fairly complicated. It involves co-precipitation of $RaSO_4$ and $BaSO_4$, subsequent dissolution, aeration and de-emanation of radon in specially fabricated scintillation cells. A similar method has been used by several other

workers (13), (17), (27). Alpha counting in a somewhat different manner was also used by some workers (28), (29).

Gamma counting is simple. Any gamma sensitive radiation detector, such as ionization chambers, scintillation counters, semiconductor counters, may be used. The only requirement is that all samples should be counted in identical sampling bottles and in identical geometries with respect to the detector. Then the count rate of different samples can be compared with the count rates of carefully prepared standards having known amounts of radium. Such a method was recently used by Seeley (12).

Fig. 3.1 shows the details of Ra^{226} decay. There are two branches in the decay of Ra^{226}. Most of the decay occurs by 4.777 MeV alpha particles.

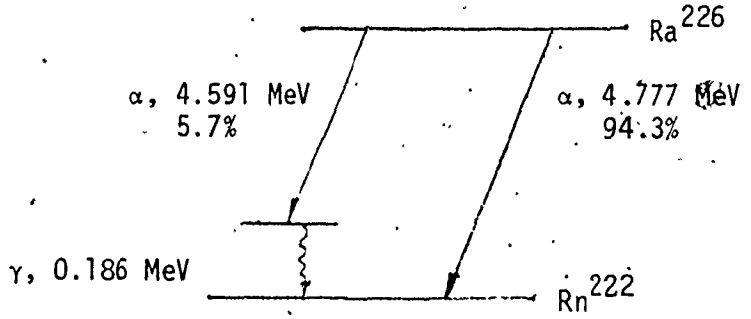

Figure 3.1 The Disintegration of Ra^{226}

Only 5.7% of the disintegrations are by 4.591 MeV alpha particles and 0.186 MeV gamma rays. The weaker branch is not given in Table 1.1 because only the highest alpha energies and prominent gamma photons from the radionuclides are listed there. If gamma counting is to be used for determination of radium, it would be desirable to count the 0.186 MeV gamma since it represents Ra^{226} directly. However, in practice, there are some drawbacks in counting the 0.186 MeV gamma peak.

(a) The 0.186 MeV gamma peak is very weak. It comes from only 5.7% of disintegrations of Ra^{226}. The count rate of this peak will be particularly low for samples with only a few picocuries of Ra^{226} which are likely to be encountered in this work.

(b) The energy of the peak (0.186 MeV) is relatively low, therefore, signal-to-background count ratio is low.

(c) The 0.180 MeV peak from U^{235} may interfere with the counts.

Due to the reasons given above, 0.186 MeV gamma counting is not a good choice even though it represents Ra^{226} directly.

It becomes, therefore, necessary to count a gamma photon from one of the decay products of Ra^{226}. From Table 1.1 it is evident that there are several gamma photons emitted by the decay products of Ra^{226}. When the count rate of such a gamma photon is measured, it is necessary to ensure that the measured count rate is representative of the amount of Ra^{226} in the sample. This can be achieved by establishing the state of secular equilibrium in the decay chain of Ra^{226}. As discussed in Chapter 1, in the state of secular equilibrium, the count rate (activity) of every member of the decay chain attains the same value. Thus, when the secular equilibrium is attained, the count rate of any of the gamma peaks from a decay product which is in equilibrium with Ra^{226}, will represent the amount of Ra^{226} in the sample. The amount of Ra^{226} in a sample can be considered constant because it decays very slowly (Half-life 1622 y).

To establish secular equilibrium, a sample must be sealed so that gaseous Rn^{222} emanating from the decay of Ra^{226} does not escape. The radon which builds-up in the sample also decays to Po^{218} and the decay process goes on according to Table 1.1. The decay products between Ra^{226}

and Pb^{210} are all relatively short-lived, Rn^{222} being the longest-lived among them (c.f. Table 1.1). The sealed sample must be allowed to come to equilibrium before counting. This is called the ingrowth period, during which the short-lived decay products attain secular equilibrium with Ra^{226} (see also Appendix B).

To summarize, a gamma counting procedure would require preparing samples in identical sampling bottles, sealing up the samples and allowing a sufficient ingrowth period before counting. The counting must be done in identical geometries with respect to the detector for every sample. The count rate of a suitable gamma peak will then represent the amount of radium in a sample which can be calibrated against count rates of standard samples with known amount of radium. The standard samples should also be exactly similar in geometry to the samples being calibrated.

3.2 GAMMA COUNTING SET-UP

Because it was straightforward and reliable, it was decided to choose gamma counting for the determination of radium in various solid and liquid samples obtained in leaching experiments throughout this work. A Ge(Li) detector was available for this purpose. Ge(Li) detectors have high resolution but poor counting efficiency. High resolution was advantageous as the gamma-ray spectrum is fairly complicated due to presence of several daughter products (with similar gamma energies) in samples.

The counting set-up used is shown schematically in Fig. 3.2a. It consists of a Ge(Li) detector and associated electronics. The principles of each of the component are briefly described in the next section. Details of the detector platform and the exact geometry in which the sample

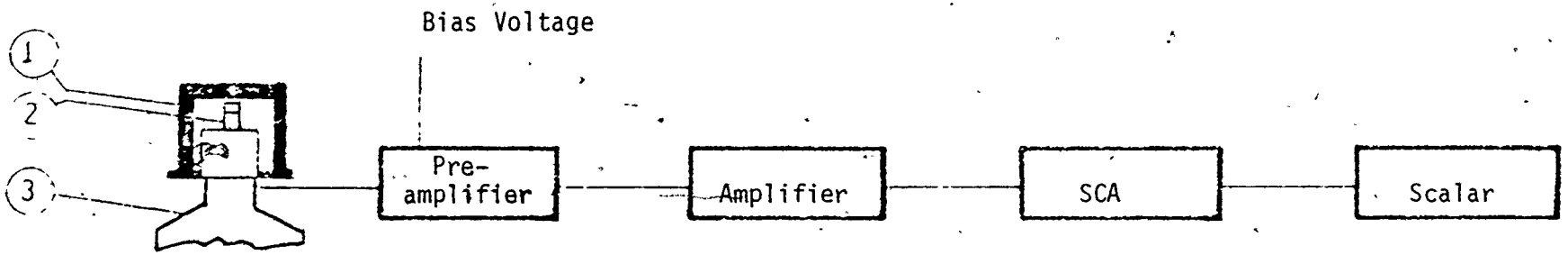

Figure 3.2a Gamma Counting Set-up with Ge(Li) Detector and Single Channel Analyzer.

(1) Lead Shielding

(2) Sample

(3) Detector

is placed with respect to the detector are given in Fig. 3.2b.

Count rates of the 609 KeV gamma peak from Bi_{33}^{214} were measured. In the early stages, a multi-channel analyzer (MCA) was used. However, later it was found to be sufficient to use a single channel analyzer (SCA). To cross-check for any possible drift in the SCA window setting, the MCA was used at regular intervale throughout the work.

Fig. 3.3 shows a typical spectrum acquired on a MCA. Some prominent peaks of the decay products (c.f. Table 1.1) can be seen in the figure. When a SCA with a scalar is used instead of a MCA, a small window encompassing the 609 KeV peak can be set on the SCA. The scalar then enables us to read the counts.

The 609 KeV gamma peak was selected for the following reasons:

(a) With only a few short-lived radionuclides between Ra^{226} and Bi^{214} in the Uranium Series, a shorter ingrowth period was necessary;

(b) The relative background level would be low at 609 KeV which is on the higher energy side of the spectrum; and,

(c) This peak is a prominent one, and is not close enough to any gamma energy in the Thorium and Actinium Series to be affected by interferences.

Specifications of the detector, associated electronics and shielding are given in Appendix A. The lead shielding helped to cut down the background count rate approximately five-fold.

3.3 BASIC PRINCIPLES OF THE COUNTING EQUIPMENT

The essence of a Ge(Li) detector is the lithium drifted germanium crystal. The lithium drifting is necessary to create a p-n junction. For

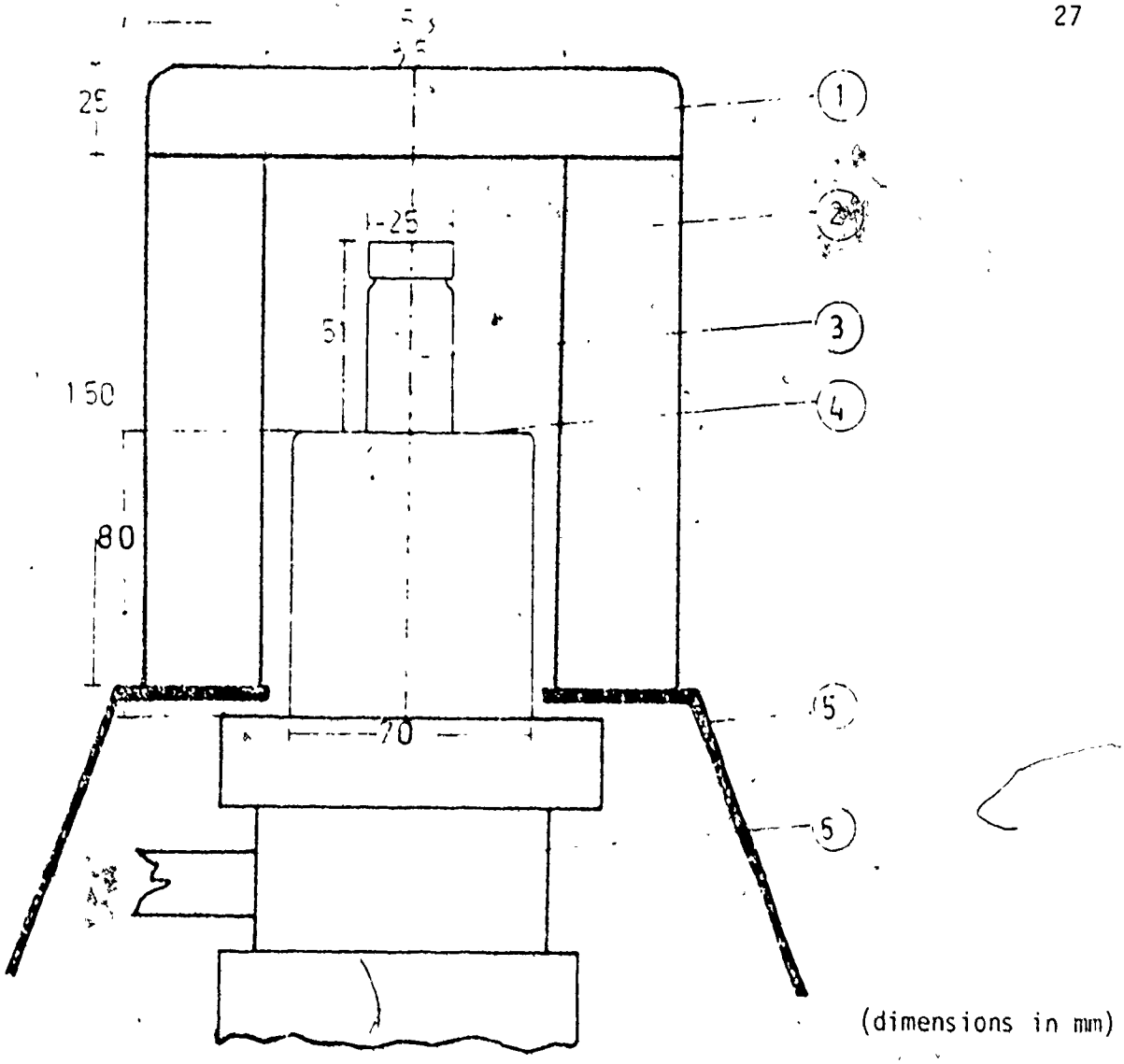

Figure 3.2b Ge(Li) Detector Platform with a Solid Sample in Place.

(1) Top Lead Cover

(2) Cylindrical Lead Shielding

(3) Solid Sample in the Vial

(4) Circular Aluminium Platform of the Detector

(5) Steel Stand

(6) Top [illegible]

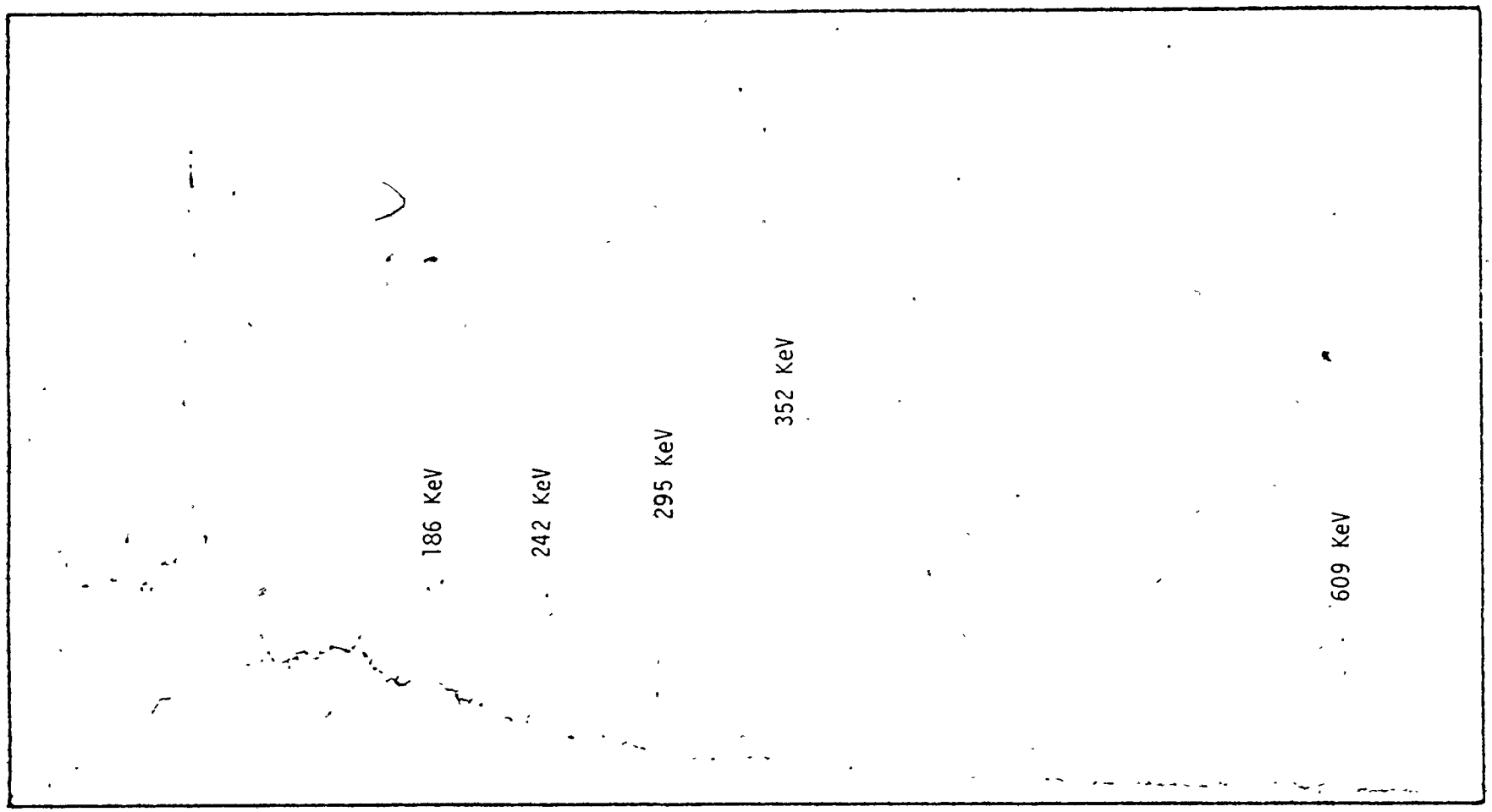

Figure 3.3 A Typical Spectrum Acquired on MCA Showing Prominent Peaks

good performance of the detector, the crystal must be defect-free. At room temperature, there are enough thermal excitations to cause electrons to migrate from the valence band to the conduction bond, spoiling the semiconducting property of the crystal. Due to this, the crystal is always kept at liquid nitrogen temperatures. Crystals of various sizes and shapes along with the attached liquid nitrogen container are commercially available.

In Fig. 3.4, the crystal is schematically shown with a high bias voltage applied. In the absence of any incident radiation, there is an extremely low steady current in the circuit because of the high resistivity of the semiconductor detector. However, when incident gamma radiations interact* with the crystal, electrons and holes are produced which move towards the appropriate electrode causing a current to flow in the circuit.

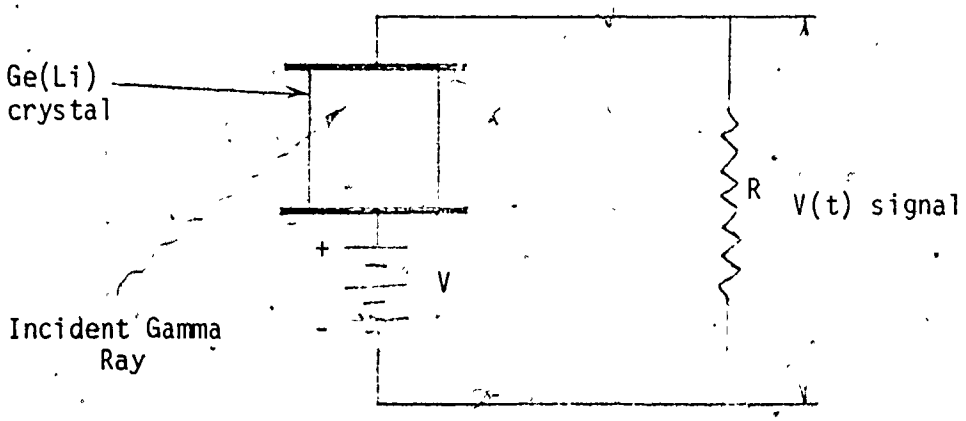

Figure 3.4 Schematic diagram of Ge(Li) detector

---

* Gamma radiations interact in several ways such as photoelectric effect, pair production, etc.

The signals from the detector are extremely weak, generally of the order of electronic noise. They are amplified carefully by a low noise-level amplifier called preamplifier. There are two types of pre-amplifiers available: charge sensitive and voltage sensitive. Charge sensitive preamplifiers are normally preferred because their amplification is independent of the capacitance of the detector itself. Once the signal is amplified sufficiently above the noise level, it can then be fed to a linear amplifier for further amplification.

Pulses amplified by the amplifier go to a single channel analyzer which is basically an energy discriminator. It can be set to accept pulses having energies within a desirable range. This is called "window" setting. If the energy of an incoming pulse falls within the set-window of the SCA, a count is registered in the scalar. No count is registered for the pulses whose energies do not fall within the energy range of the SCA window.

A MCA is far more versatile than a SCA. In Pulse Height Analysis (PHA) mode, a MCA receives pulses from a detector and amplifier. These pulses have amplitude (height) which vary in proportion to the energies of incident radiations absorbed by the detector. By counting the number of occurrences of each height and forming a histogram, a MCA measure the energy spectrum as seen by the detector. The entire energy spectrum is divided into successive steps and the occurrences are, in fact, counted in each of these energy channels. Besides this, a MCA has analog to digital converter, solid state memory, Cathode Ray Tube display unit and input/output circuitry.

Since count rate of 609 KeV peak alone was to be measured, a SCA can be used instead of a MCA. It is necessary to set the "window" of the SCA corresponding to the desired peak (609 KeV in this case). This can be done by obtaining the whole spectrum on the MCA first (c.f. Fig. 3.3) and setting upper and lower limits of SCA window corresponding to the channel numbers which encompass the peak on MCA spectrum.

3.4 EXPERIMENTAL ASPECTS

3.4.1 Procedure: Bench scale leaching experiments were carried out in 1 ℓ glass beaker, 14 cm in height and 10 cm in diameter. A known amount of tailings* were contacted with a known amount of extractant for a certain time. Each batch was continuously stirred by a teflon-coated magnetic stirring bar (length 40 mm, dia. 8 mm). For total suspension of tailing particles, a stirring speed of approximately 500 rpm was necessary. To avoid any evaporation loss, the beaker was covered during each leaching run.

At the end of each run, the mixture (tailings + extractant) was quickly filtered in a Büchner funnel. After filtration, the wet solids (with adhering liquid) were weighed to account for the adhering liquid. In most cases, the wet solids weighed about 20% more than dry untreated tailings.

Samples were prepared (see section 3.4.4) from the wet solids

* From now on the word "tailings" will mean the dried solids from the tailing-line of Rio Algom's Elliot Lake uranium operations. Two shipments of such tailings were received each having different radium content.

and the filtered liquid. These samples were subsequently counted to find the count rate of the 609 KeV gamma peak.

3.4.2 Planning the Leaching Experiments: Results of radium analysis by gamma counting became available a minimum of 40 days after the date of the leaching experiment because of the ingrowth period. It was, therefore, necessary to plan leaching experiment for various extractants in a systematic manner.

Counting results in the early stages of the work indicated that radium is leached out fairly quickly from the tailings. It took less than half an hour of the leaching to reach an equilibrium radium concentration in the liquid phase for some extractants like EDTA and $CaCl_2$ solutions. Based on these observations, subsequent leaching experiments were of two kinds.

(a) Equilibrium Runs: Several leaching experiments with different solid-to-liquid ratios were carried out for a fixed period of time - usually more than 2 hours.

(b) Kinetic Runs: A reasonable solid-to-liquid ratio was chosen and the leaching experiments were carried out for different times of contact - varying from 15 minutes to 18 hours, each in a separate batch.

3.4.3 Untreated Tailings: The following experiments were carried out with the untreated tailings which were received in two shipments.

(a) Several representative samples of untreated tailings were prepared from each shipment. These samples were counted after the ingrowth. This gave average values of radium content in each case.

(b) Sieve Analysis was carried out separately for both the shipments.

Standard Tyler Sieves were used for this purpose. The activity of radium in each size fraction was measured by the counting procedure. These experiments were necessary to observe the distribution of radium with regard to particle size.

3.4.4 Sample Preparation: Radium content in the liquid samples was expected to be in the order of a few tens of picocuries per gram whereas the wet solids would be considerably higher in radium concentration. For this reason, liquid sampling bottles were selected to be of much larger capacity. With the larger amount of liquid contained in the sampling bottle, a good count rate could be achieved. For solid samples, however, small vials served the purpose.

For solid samples, 20 ml Kimble glass vials with 'Poly Seal' screw caps were used. Liquid samples were prepared in 115 ml flint glass, squat form sampling bottles with screw caps. Exact dimensions and drawings of sample bottles of each kind is given in Fig. 3.5. When filled up to a predetermined mark in either case, samples are expected to be of identical geometry. Enough care was taken to ensure identical positioning of each sample with respect to the detector at the time of counting.

Every sample must be sealed properly so that Radon gas which builds up in the sample due to decay of Ra^{226} may not escape. Commercially available refined wax was used to seal every sample at its lid. Due to decay of Radon, Bi_{83}^{214} whose 609 KeV gamma peak is being counted, should grow exponentially to its equilibrium value. In practice an ingrowth time of about 40 days (12) (Appendix B) (more than 10 half-lives of Rn^{222}) was sufficient to ensure equilibrium values of the count rate.

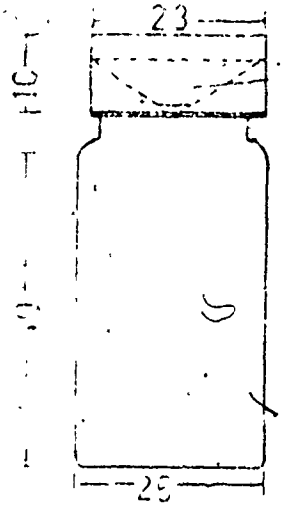

Figure 3.5a 20 ml Capacity Glass Vial for Solid Samples

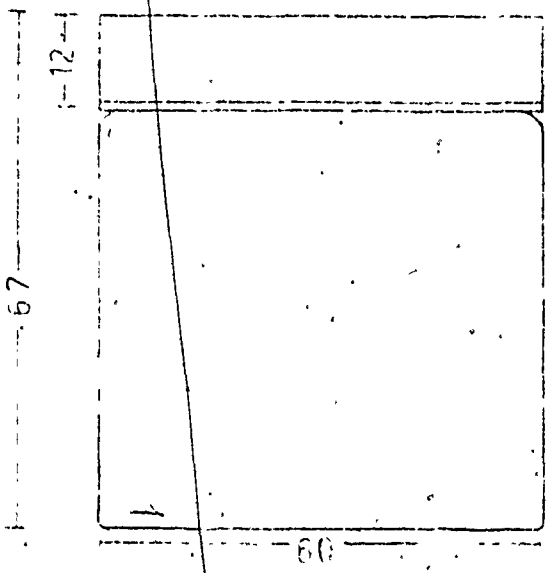

Figure 3.5b 115 ml Capacity Flint Glass Bottle for Liquid Sample

(Dimensions in mm)

3.5 PREPARATION OF STANDARDS AND CALIBRATION

Solid and liquid standards were prepared with Gamma Ray Radium Standards available from National Bureau of Standards (NBS), Washington. The NBS standards have a known amount of radium dissolved in a precisely weighed solution. The same glass vials and flint glass bottles used for the samples (described in the previous section) were also used to prepare solid and liquid standards.

A known amount of NBS standard solution was carefully transferred into a weighed amount of ordinary beach sand (of the same average particle size as that of the tailings). The two were well mixed and the mixture was dried at room temperature. Later, different amounts of this radium-soaked sand was put in different vials. Since the total weight of the mixture and its radium content was known, the amount of radium put in different vials was also known by calculation. To fill up each vial up to the predetermined mark, an extra supply of ordinary beach sand was used. The ordinary beach sand was thoroughly mixed with the radium soaked sand. The samples were then sealed, allowed to grow in and counted in the usual manner. Solid standards containing about 1300 pCi to 12000 pCi radium were prepared in this manner.

For the liquid standards, different amounts of the original NBS solution were transferred into different liquid sample bottles. Distilled water was used to make up the required concentrations. Liquid standards containing about 500 pCi to 3500 pCi were prepared in this fashion.

These liquid and solid standards were counted and calibration curves of True Counts per hour against Radium Content (pCi) were obtained. These curves were used to determine radium content (and hence radium in

pCi/g as every sample was precisely weighed) of the various solid and liquid samples obtained.

3.6 STATISTICAL CONSIDERATIONS

Statistical errors are always associated with a counting procedure because of the random nature of the radioactive disintegration. In most cases, the errors introduced in taking the counts and in the measurement of time intervals are negligible compared to the statistical error.

The binomial distribution describes the random events of radioactive decay. When counting time is very small compared to the half-life of the radioactive atom (i.e., $\lambda t << 1$), the binomial distribution law gives

$$\sigma = m^{1/2} \simeq (\bar{n})^{1/2}$$

where σ, m and $\bar{n}$ are the standard deviation, true mean and average number of counts, respectively. m and $\bar{n}$ are usually not known. Instead, a single measurement of n counts in a time interval t is made.

The standard deviation is frequently used as precision index in counting. The counts are reported as $n \pm n^{1/2}$, assuming $n \simeq \bar{n} \simeq m \simeq \sigma^2$. For a single measurement of n counts taken over a time interval t, the count rate r is given by

$$r = \frac{n}{t}$$

In terms of the standard deviation

$$r \pm \sigma_r = \frac{n}{t} \pm \frac{n^{1/2}}{t} = r \pm \frac{r}{n^{1/2}}$$

The above expression, stated in terms of % error in r, becomes

$$r \pm \frac{100}{n^{1/2}} \%$$

Thus n should be infinitely large for an accurate determination of r. In practice, a compromise is made depending on the availability of counting time. For this work, a percentage error of about 3% was considered reasonable. Therefore, each sample was counted for at least 1000 counts. The count rates of most solid samples were high enough so that 1000 counts were attained in a reasonable time interval (a few tens of minutes), however, some liquid samples with extremely low radium concentration took as much as half a day to count.

CHAPTER 4

PRELIMINARY WORK

Some preliminary work on background counting, calibration, activity of untreated tailings, sieve analyses, and ingrowth of samples is reported in this chapter. This information will be frequently used in calculations and interpretation of results of the leaching experiments, which are discussed in the next chapter. Use of the counting set-up for the preliminary work was helpful in establishing the validity of the analytical technique.

4.1 BLANK SAMPLES

Blank solid and liquid samples were prepared to measure background count rates in the counting set-up. Ordinary beach sand of appropriate particle size was used to prepare the solid blank samples. Liquid blanks were prepared using distilled water in the flint glass sample bottle.

The background count rate should be sufficiently low compared to the count rates of different samples obtained in the work. As pointed out earlier, the lead shielding cut down the background count rate approximately five-fold. Since the background count rate is low, it is necessary to count it for a longer time to reduce statistical variation. This was done by counting the background overnight several times. No significant difference in the background counts for the solid and liquid blanks were observed and the count rate remained fairly constant. The

count rate for both the cases (solid as well as liquid blanks) remained close to 190 counts/hr throughout the work.

4.2 THE CALIBRATION CURVES

The calibration curves, in counts per hour* plotted against radium content of different standard samples (c.f. section 3.5) in picocuries (pCi) were obtained by counting the standards after the ingrowth period. Tables 4.1-4.3 give the data for 1) solid standards in scintillation vials, 2) liquid standards in flint glass sample bottles and 3) liquid standards in scintillation vials, respectively. The data include the known radium content in pCi, amount of each standard after addition of make-up sans or distilled water, and the count rates. Corresponding curves are plotted in Fig. 4.1-4.3. It should be noted that weight of every standard with make-up sand or water in a particular category (1, 2 or 3 above) is approximately the same (see 3rd column in Tables 4.1-4.3). Since approximately the same amount of material (solid or liquid, as the case may be) is filled in bottles of certain shapes and sizes, it will build-up similar geometries. The straight line calibration curves (Fig. 4.1-4.3) can be explained because counts/hr (ordinate) and pCi radium (abscissa) are "definition" of each other.** In other words, counts/hr is expected to increase proportionately with the amount of radium in picocuries. Any scatter observed is attributed to experimental errors in weighing,

---

* The count rate reported in various tables are rounded off to the closest whole number after correcting for the background count rate.

** One Curie (Ci) by definition is 3.7×10^{10} disintegrations per second.

Table 4.1 Data for the calibration of solid samples in scintillation vials

Sample Code	Radium content (pCi)	Amount, g (with make up sand)	Counts/hr
SS-1	1362	35.4656	355
SS-2	2171	35.2039	625
SS-3	3163	33.3463	821
SS-4	3952	33.4276	1228
SS-5	4434	33.2360	1381
SS-6	4981	33.6711	1274
SS-7	6152	37.0699	1790
SS-8	10046	37.3209	3046
SS-9	12185	37.6004	3484

Table 4.2 Data for the calibration of liquid samples in flint glass sampler

Sample Code	Radium content (pCi)	Amount, g (with make up water)	Counts/hr
LS-1	698	109.85	71
LS-2	1631	112.09	233
LS-3	1800	111.35	245
LS-4	2374	110.94	336
LS-5	2813	110.82	394
LS-6	3024	107.07	390

Table 4.3 Data for the calibration of liquid samples in scintillation vials

Sample Code	Radium content (pCi)	Amount, g (with make up water)	Counts/hr
S-1	808	21.37121	198
S-2	1586	20.1128	412
S-3	2361	20.5357	604
S-4	3328	20.5119	859

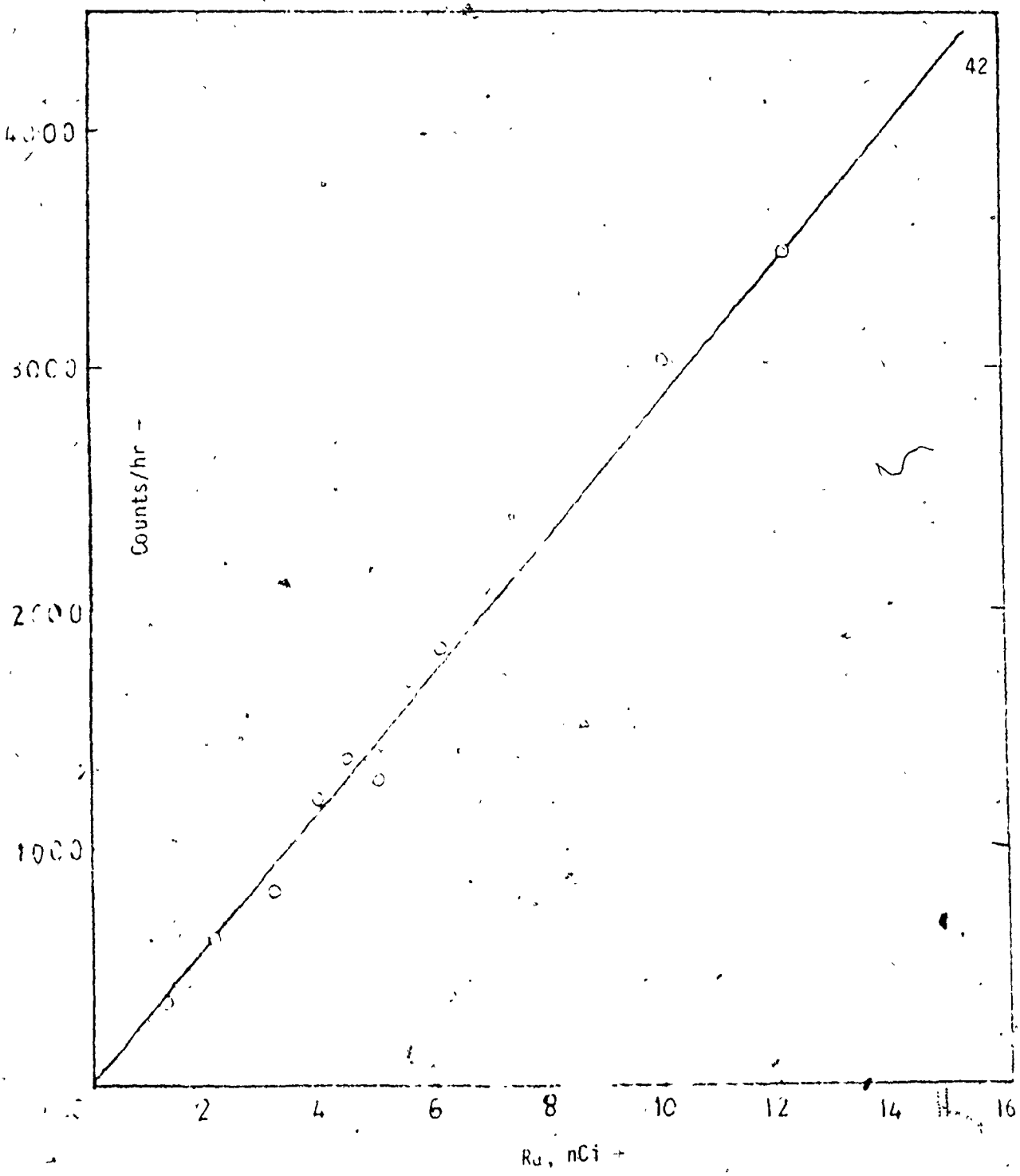

Figure 4.1 Calibration of Solid Samples in Scintillation Vials (counted in a fixed geometry)

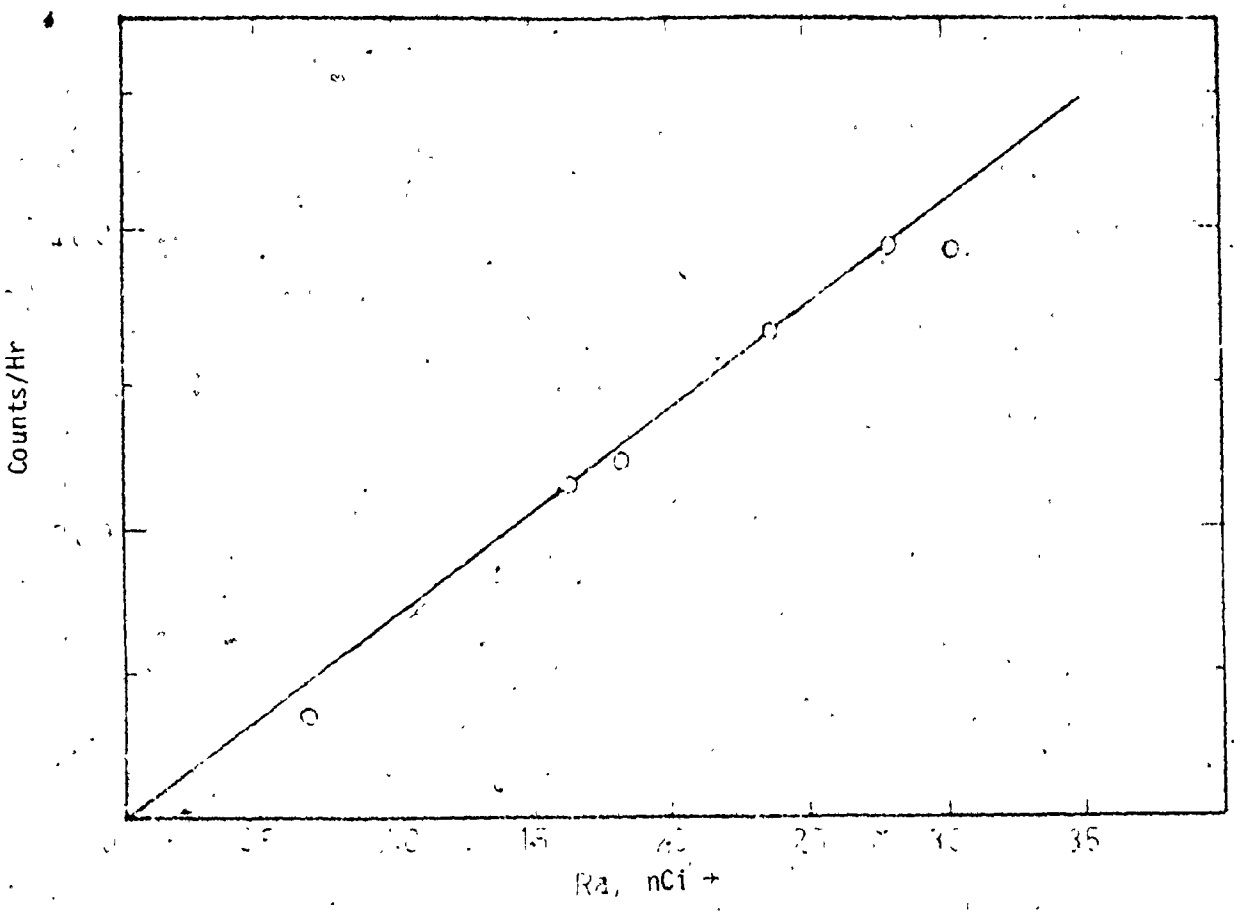

Figure 4.2 Calibration of Liquid Samples in Flint Glass Bottles (counted in a fixed geometry)

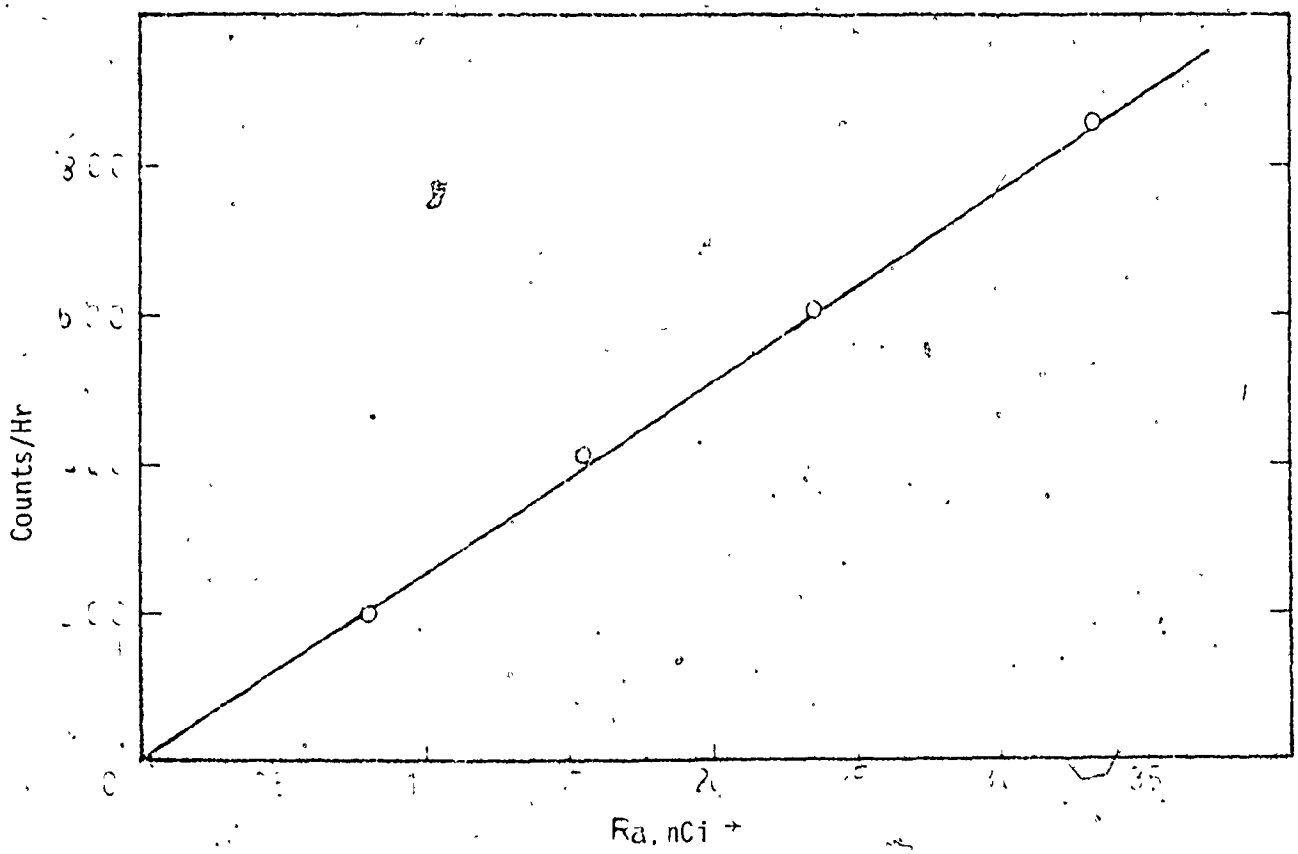

Figure 4.3 Calibration of Liquid Samples in Scintillation Vials (counted in a fixed geometry)

mixing and evaporating (for solids) and in transferring very small amounts of solutions from the original NBS solutions.

The difference in the slopes of the straight lines for different types of standard is due to the differences in the size, shape and self-shielding effects. It can be noted that slopes for standards of type 1) and 3) above are close enough indicating that self-shielding effects in solid and liquid are reasonably close to each other (c.f. Appendix C).

4.3 ACTIVITY OF THE TAILINGS

Several representative samples of the tailings were prepared from both the shipments received. Table 4.4 gives the amounts contained in different samples, count rates and radium concentrations in picocuries per gram (pCi/g). The values in pCi/g were obtained from the calibration curves and the known amounts of sample. Average values were taken for the concentration of radium in each case for all subsequent calculations.

4.4 SIEVE ANALYSES

The tailings of the two shipments were collected at two different points in the tailing line of the uranium mill, The average particle size was smaller for the tailings received in the second shipment. The radium content was also substantially different in the two (c.f. Table 4.4), however, the range of particle size was roughly the same. Tables 4.5-4.8 summarize the data on sieve analyses.

In both cases, the weight percentage for different size fraction was the average of three different sieving experiments, starting with different initial masses of the tailings. Radium content of each of the

Table 4.4 Counting data on the representative samples from two different shipments of Mill-tailings

Shipment	Sample Code	Amount, g	Counts/hr	Radium Content pCi/g
First	T-1	28.1104	2910	371.04
	T-2	22.1656	2413	381.02
	T-3	22.7218	2499	384.94
	T-4	22.21455	2588	406.96
	T-5	21.16715	2588	427.93
				Average = 394.378
Second	T-6	18.76378	4018	749.48
	T-7	20.55725	4545	773.81
	T-8	20.7972	4601	774.31
	T-9	18.3505	4284	817.09
	T-10	20.28232	4215	727.36
				Average = 768.410

Table 4.5 Differential Sieve Analysis on Tailings Received in the First Shipment

Sample Code	Mesh	Screen opening mm (range)	Average Weight %	Sample Weight, g	Radium Content pCi/g	Radium %
A	30/50	0.600-0.297	2.96	19.178	369.199	2.67
B	50/100	0.297-0.150	18.13	24.970	244.974	10.85
C	100/140	0.150-0.105	16.04	25.742	247.455	9.70
D	140/200	0.105-0.075	17.13	24.351	269.783	11.29
E	200/230	0.075-0.063	12.11	16.369	637.821	18.87
F	230/Pan	0.063-smaller	33.63	15.577	567.343	46.62
			100.00%			100.00%

Table 4.6 Integral Sieve Analysis on Tailings Received in the First Shipment

Sample Code	Mesh	Particle Size* mm (larger than)	Cumulative Fraction (Undersize) Weight	Radium
	30	0.600	0.0	0.0
A	50	0.297	0.0296	0.0267
B	100	0.150	0.2109	0.1352
C	140	0.105	0.3713	0.2322
D	200	0.075	0.5426	0.3451
E	230	0.063	0.6637	0.5338
F	Pan	0.000	1.0	1.0

* "Particle size" is expressed here in terms of the dimensions of the mesh holes which just permit the particles to pass.

Table 4.7 Differential Sieve Analysis on Tailings Received in the Second Shipment

Sample Code	Mesh	Screen opening mm (range)	Average Weight %	Sample Weight, g	Radium Content pCi/g	Radium %
A-1	30/50	0.600-0.297	5.8	21.501	708.917	5.69
B-1	50/100	0.297-0.150	10.1	19.688	636.330	8.90
C-1	100/140	0.150-0.105	7.5	20.857	656.025	6.81
D-1	140/200	0.105-0.075	14.9	20.742	621.081	12.81
E-1	200/230	0.075-0.063	14.9	18.988	689.556	14.22
F-1	230/270	0.063-0.053	6.6	18.666	729.122	6.67
G-1	270/Pan	0.053-smaller	40.2	17.019	806.607	44.90
			100.00%			100.00%

Table 4.8 Integral Sieve Analysis on Tailings Received in the Second Shipment

Sample Code	Mesh	Particle Size* mm (larger than)	Cumulative Fraction (Undersize) Weight	Radium
	30	0.600	0.0	0.0
A-1	50	0.297	0.058	0.0569
B-1	100	0.150	0.159	0.1459
C-1	140	0.105	0.234	0.2140
D-1	200	0.075	0.383	0.3421
E-1	230	0.063	0.532	0.4843
F-1	270	0.053	0.598	0.5510
G-1	Pan	0.0	1.0	1.0

* "Particle size" is expressed here in terms of dimensions of the mesh holes which just permit the particles to pass.

samples was calculated using the calibration curves. The percentage of radium was calculated as follows

$$\text{Radium \%} = \frac{\text{picocuries appearing in a certain size fraction}}{\text{picocuries of initial tailings mass}} \times 100$$

As expected, the weighted average of radium content in different size fractions balanced very well with the radium input. In the two cases of sieve analyses discussed above, the mass balance gave 104% and 94% of the input radium. The differential and integral sieve analyses results are graphically presented in Fig. 4.4 and 4.5, respectively.

The radium content in pCi/g generally increased as the particle size decreased, though there are some deviations from this. For example, sample A of the first shipment is considerably higher in radium content as compared to Samples B, C and D (c.f. Table 4.5). This could be explained if the particles of the 30/50 mesh size are actually made up of an agglomeration of finer particles. To check on this hypothesis, an electron microscopic photograph of the surface of a 30/50 mesh size was taken (Fig. 4.6). The photograph shows that there are in fact, extremely fine particles which agglomerate to form the bigger particle. This finding was very interesting but somewhat outside our main line of investigation and hence was not pursued further.

4.5 INGROWTH STUDY ON SOLID SAMPLES

The sieve fractions of the first shipment (samples A-F) were counted several times during their growing in period to observe how the count rate and relative activity varies during this period. Relative activity is defined here as follows:

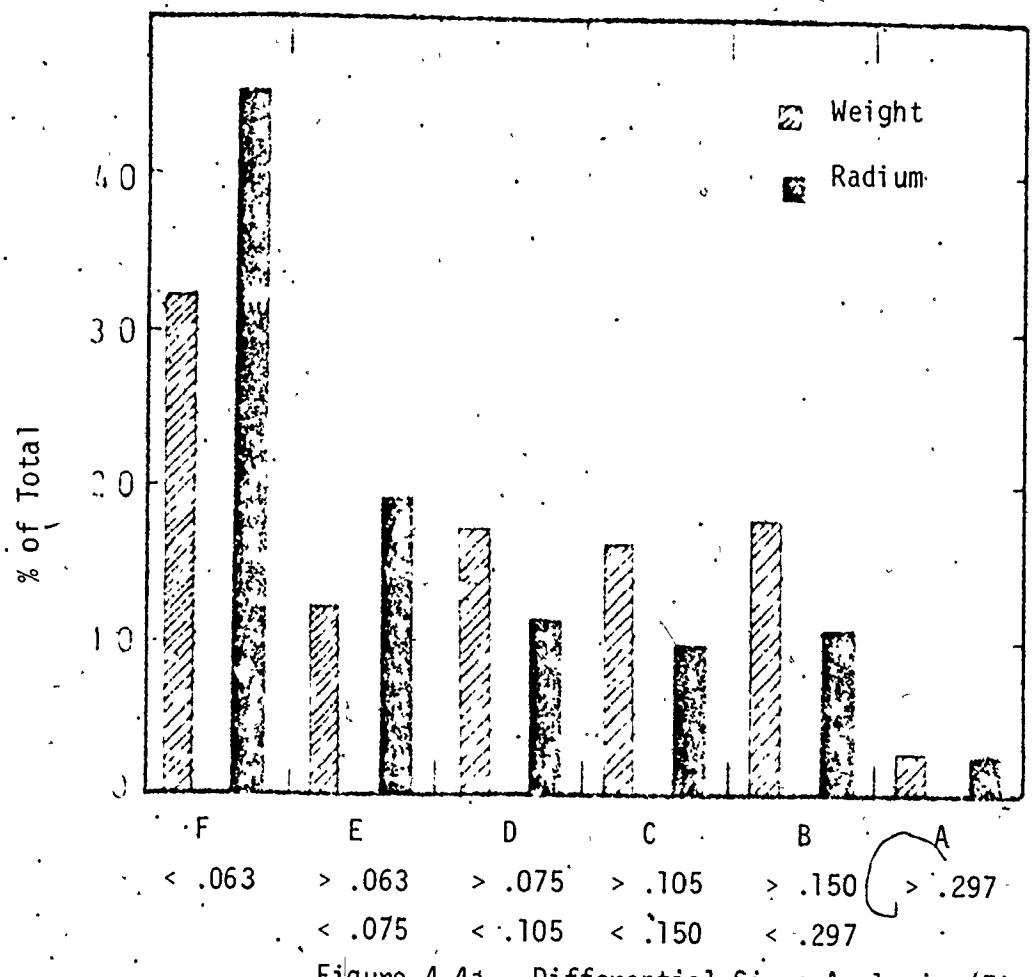

Figure 4.4a Differential Sieve Analysis (First Shipment)

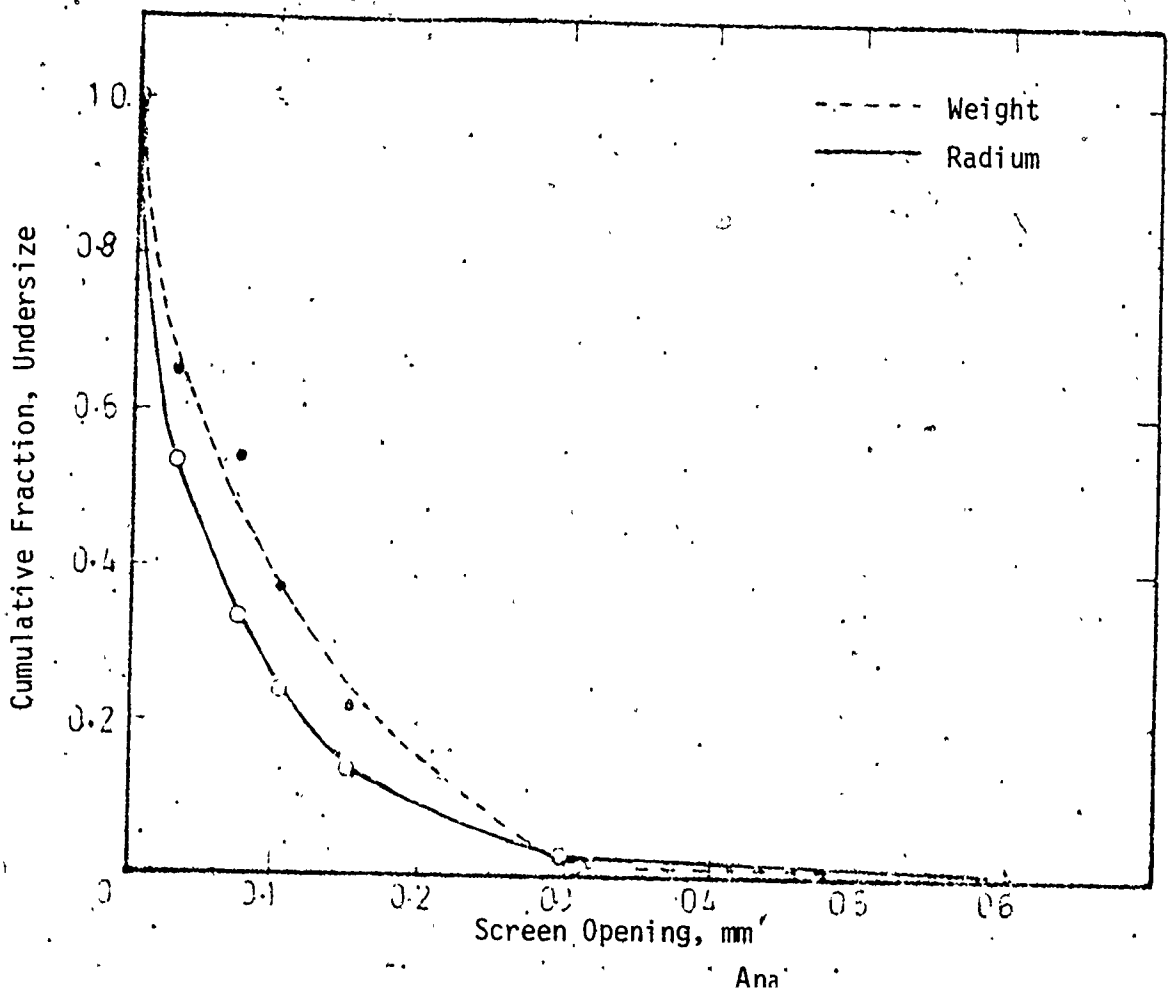

Ana

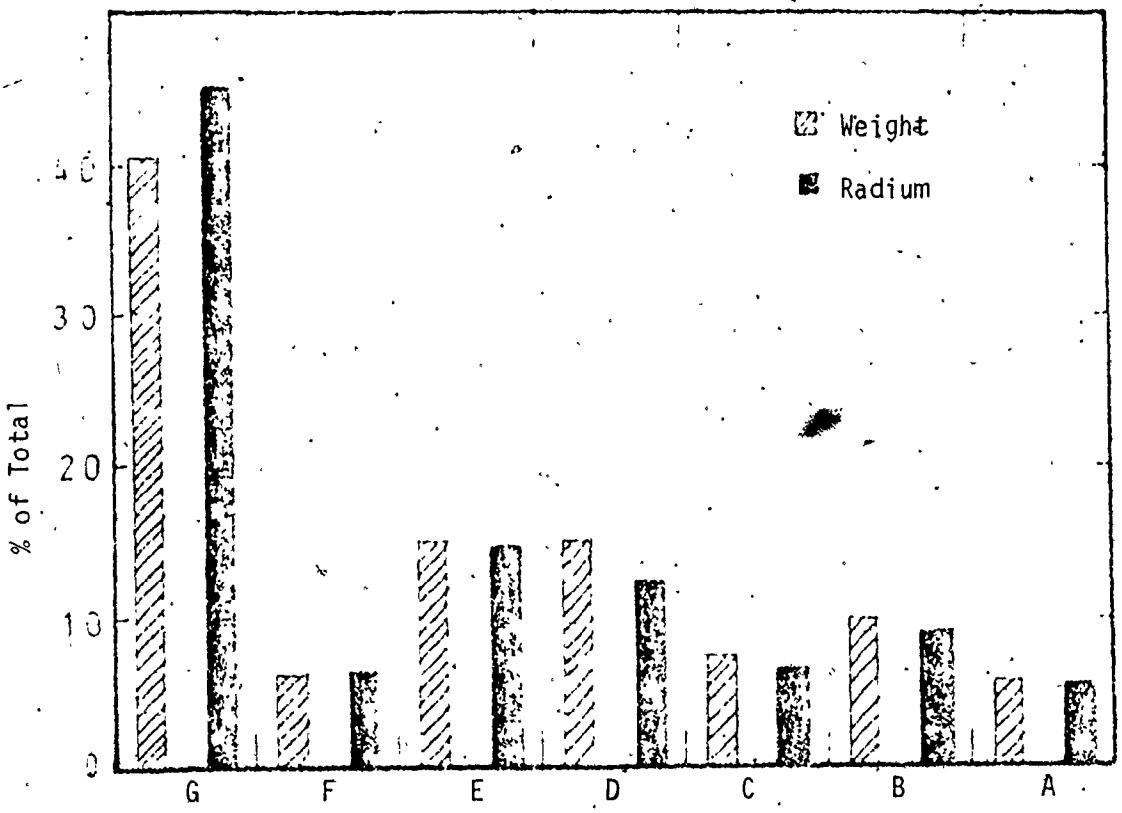

Figure 4.5a Differential Sieve Analysis (Second Shipment)

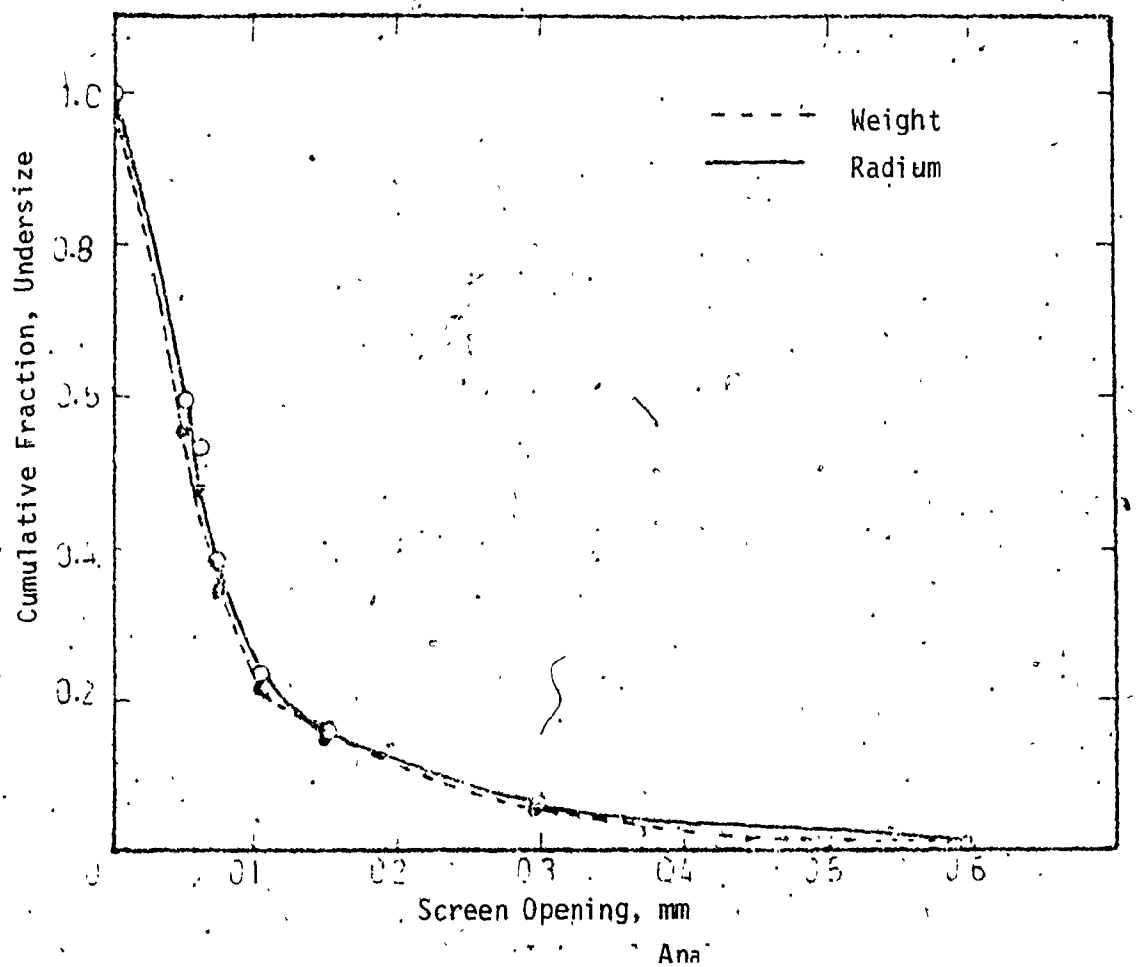

Ana

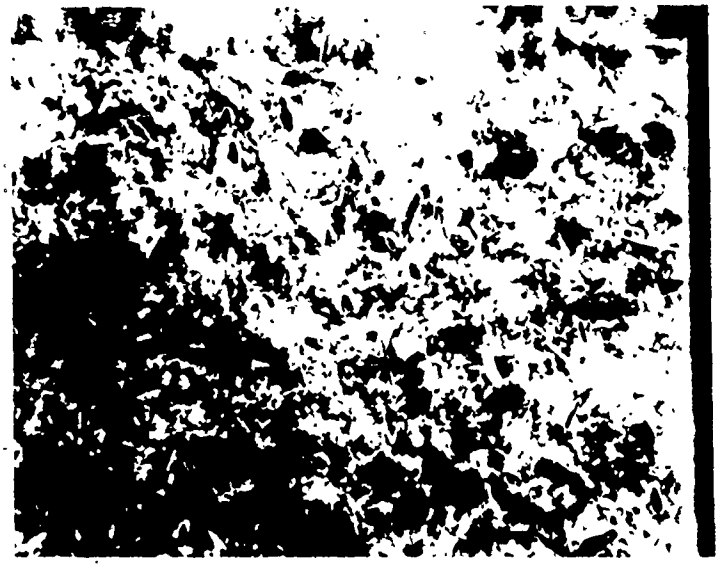

Figure 4.6 Electron Microscope Photograph (x 470) of a particle of 30/50 Sieve fraction from the first shipment. The dark dots represent finer particles which constitute the (bigger) particle. A typical dark dot is about 3 mm in size. Thus, the actual size, 3/470 = 0.0063 mm, is finer than the smallest size sieve fraction.

$$\text{Relative Activity} = \frac{\text{count rate at anytime during ingrowth period}}{\text{count rate after 40 days of ingrowth}}$$

Table 4.9 shows the count rate and relative activity (R.A.) with time after sealing a certain sample. The average values of relative activities at different times is calculated to smooth out statistical and background fluctuations and effects due to slight differences in geometry which were beyond control (e.g., packing factor in the sample bottle). In Fig. 4.7 relative activity is plotted against number of Rn^{222} half-lives. The ingrowth pattern in approximately exponential as expected (c.f. Appendix B). The vertical bars indicate the fluctuations in relative activities of different samples about the average value.

This study proves how Bi^{214} (whose 609 KeV gamma is counted) builds up to an equilibrium value with time after a particular sample is sealed off. The equilibrium period is about 40 days (i.e., about ten half-lives of Rn^{222}). Since a state of secular equilibrium is attained after this period, the count rate of 609 KeV gamma, for example, is representative of radium content of the sample.

Table 4.9: Count Rates and Relative Activities of Some Solid Samples during Ingrowth Period

Time After Sealing (days)		0.5	3.5	7.5	12	16	24	33	38	46
Half-Lives of Rn^{222}		0.13	0.92	1.97	3.16	4.21	6.32	8.68	10	12.10
Sample Code										
A	Count Rate	1170	1524	1891	2089	2150	2229	2010	2130	2023
	R.A.	0.5783	0.7533	0.9347	1.0079	1.0627	1.1018	0.9935	1.0529	1.0
B	Count Rate	1106	1235	1596	1621	1785	1873	1625	1614	1747
	R.A.	0.6330	0.7069	0.9136	0.9279	1.0218	1.0721	0.9302	0.9239	1.0
C	Count Rate	1174	1334	1643	1750	1760	1868	1740	1749	1820
	R.A.	0.6450	0.6725	0.9027	0.9615	0.9670	1.0263	0.9560	0.9610	1.0
D	Count Rate	1116	1309	1671	1763	1911	1854	1861	1944	1877
	R.A.	0.5946	0.6974	0.8903	0.9393	1.0181	0.9877	0.9915	1.0357	1.0
E	Count Rate	1556	2009	2383	2571	2659	2788	2601	2783	2983
	R.A.	0.5216	0.6735	0.9665	0.8619	0.8914	0.9346	0.8719	0.9330	1.0
F	Count Rate	1450	1917	2280	2456	2459	2668	2428	2485	2525
	R.A.	0.5742	0.7592	0.9030	0.9727	0.9739	1.0566	0.9616	0.9842	1.0
Average	R.A.	0.5911	0.7105	0.9185	0.9452	0.9891	1.0298	0.9508	0.9818	1.0

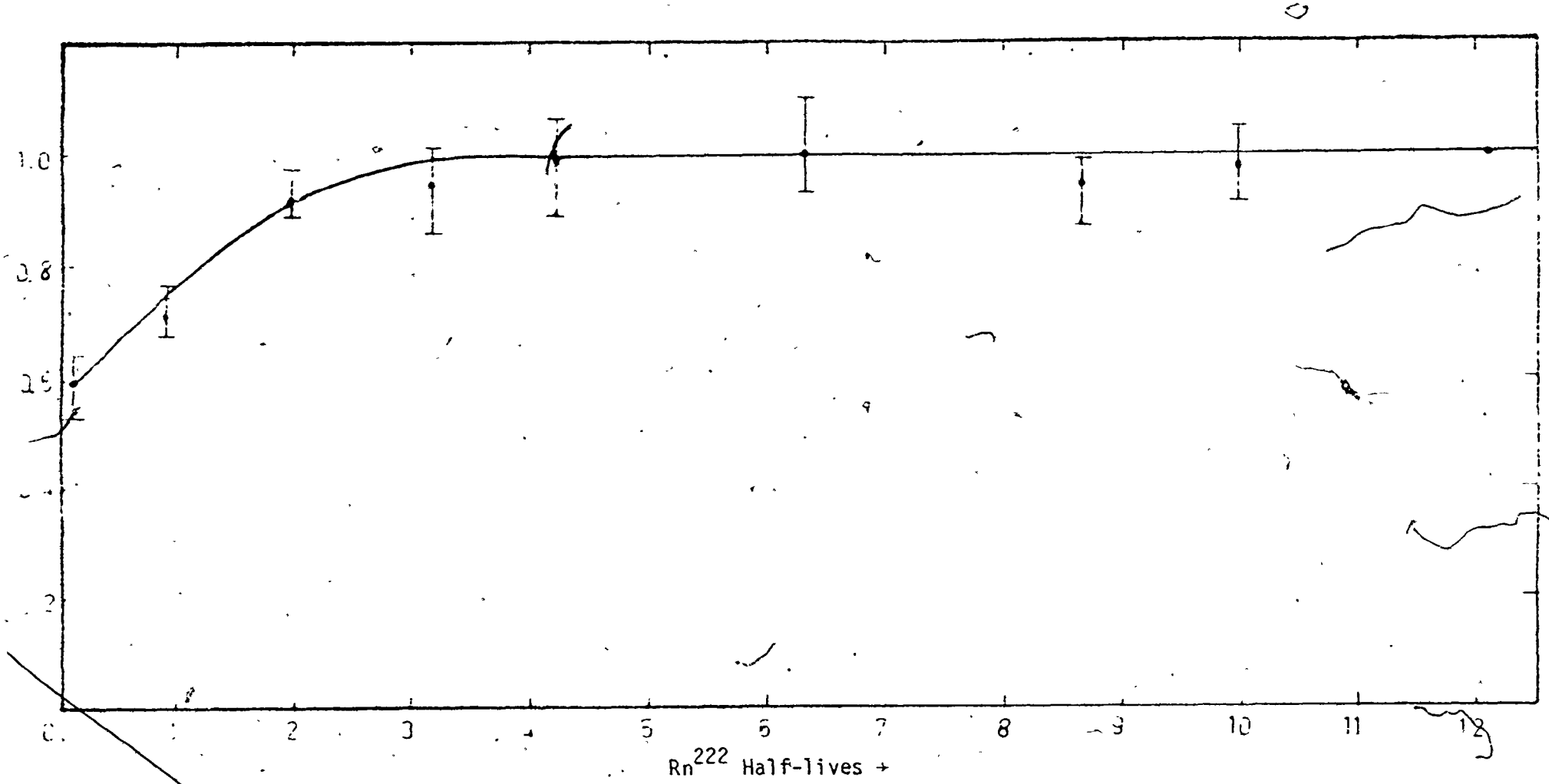

Figure 4.7 Average Growth of Solid Sieve Samples.

CHAPTER 5

EXTRACTION OF RADIUM

This chapter is about leachability of radium in some extractants. Two kinds of experiments were performed with each extractant: 1) Equilibrium Runs; and, 2) Kinetic Runs. The results are tabulated and interpreted. A limited number of additional experiments were also performed to determine the effect of concentration of the extractant and cross current contacting.

5.1 LEACHING STUDIES ON THE TAILINGS

5.1.1 Theory: Suppose S g of solid tailings (radium content x_0 pCi/g) are leached with L g of extractant and we get S' g of solids with liquid adhering and $(L + S - S')$g of liquor at the end of leaching. Let the activity of radium in wet solids be x' pCi/g and in the liquid phase be y pCi/g When the activity of the wet solids is corrected to a dry basis, it is x pCi/g.

Leaching and subsequent counting experiments were performed so that S, L, S', x', y and x_0 are known quantities. A simple radium mass balance gives

$$Sx_0 = Sx + Ly \tag{1}$$

For the wet solids

$$S'x' = Sx + (S'-S)y \tag{2}$$

To calculate x, i.e., pCi/g for the solids on a dry basis, we get

from (2)

$$x = \frac{S'}{S}(x'-y) + y \qquad (3)$$

The ratio S'/S is always greater than one. There are two ways in which the fractional removal of radium by the extractant can be defined:

From dry solid concentration

$$Fr_1 = 1 - \frac{x}{x_0} \qquad (4)$$

and from the concentration of liquid phase

$$Fr_2 = \frac{Ly}{Sx_0} \qquad (5)$$

It can be easily shown that $Fr_1 = Fr_2 = Fr$.

Let the equilibrium relation be

$$y = m(x - x_N) \qquad (6)$$

where x_N is a constant. The physical significance of x_N is that there is always some residual radium in the solids after leaching.*

Substituting y from Eqn. (6) in Eqn. (1) and simplifying

$$x = \frac{Sx_0 + mLx_N}{S + mL} \qquad (7)$$

---

* This will be evident from the data. This form of the equilibrium relation best explains the experimental results.

From Eqn. (4)

$$Fr = 1 - \frac{x}{x_o} = \frac{mL(x_o - x_N)}{x_o(S+mL)} \qquad (8)$$

or

$$\frac{1}{Fr} = \frac{x_o}{x_o - x_N}\left[1 + \frac{S}{mL}\right] \qquad (9)$$

If $\frac{1}{Fr}$ is plotted against $\frac{S}{L}$ a straight line with intercept $\frac{x_o}{x_o - x_N}$ and slope equal to $\frac{x_o}{m(x_o - x_N)}$ must be obtained. Clearly $\frac{x_o}{x_o - x_N}$ should always be greater than one for positive x_N. Also as $S/L \to 0$, $F_r \to \frac{x_o - x_N}{x_o}$. Let this limiting value be called Fr* which is the maximum extractable fraction.

5.1.2 Practical Aspects: In an actual leaching experiment, the radium mass balance (Eqn. (1)) is not perfectly satisfied because of experimental and statistical errors. A convenient way is to define radium accountability, A as follows

$$A(Sx_o) = Sx + Ly \qquad (10)$$

Ideally, A should be unity. If A is different from unity, the fraction removed, Fr_1 and Fr_2, will not be equal. For the purpose of calculations and interpretation Fr_2 defined by Eqn. 5 is accepted.

Since x_o is the average value of several tailing samples, it is reasonable to assume it to be quite accurate. The calculated value of x depends on both x' and y (Eqn. 3). Thus, when Fr_2 is accepted, the error is mainly due to measurements of y, whereas if Fr_1 was accepted, uncertainties in both x' and y matter.

Purely on statistical grounds, x' values could be measured more accurately as solid samples gave much higher count rates compared to liquid samples in general. However, there are several other uncertainties and errors in calibration of solid samples which make y values more acceptable. Some inevitable uncertainties and errors introduced in the measurement of x' are explained below:

(a) Packing Density: It was very difficult to ensure identical packing density for all solid samples. Some samples are stuffed more tightly in the vials compared to others. Such differences among various samples and the differences of an individual sample with the standards introduce errors in calibration by gamma counting.

(b) Wetness of the Solid Samples: The ratio S'/S could not be held constant for all the solid samples therefore some samples were wetter than others. The ratio also varied from one extractant to another. Wetness of the solid standards was certainly different. The wet solids from leaching experiments were "cake-like", whereas the standards were powder-like solids, since only very small amounts of original radium solution had to be added to the blank beach sand to prepare solid standards.

(c) Texture of the Wet Solids: The texture of tailings changed with prolonged leaching in corrosive liquids (e.g., HNO_3) and continuous grinding by the stirrer. In other words, wet solids from 18 hrs of leaching, for example, were quite different in characteristics than wet solids from 15 min of leaching.

(d) Erosion: Slow erosion of the teflon stirrer and the bottom surface of glass beakers was observed in prolonged leaching experiments.. Presumably, the eroded particles stayed with the wet solids after filtration, thereby introducing error in determination of radium content per gram.

Due to this reasoning, Fr_2 was accepted to be more accurate than Fr_1. Fr_2 will be referred to as Fr from now on and will be defined by eqn. (5).

5.2 EQUILIBRIUM RUNS

These experiments were meant to investigate the effect of varying solid to liquid ratio on the extraction of radium. The time of contact to ensure equilibrium was decided by the results of kinetic runs which will be discussed in the next section. In the actual experiments, the equilibrium runs were done only after analyzing the results of the corresponding kinetic runs. In all the cases, a contact time of about 2 to 3 hrs was considered adequate to ensure equilibrium.

The results from these experiments are given in Tables 5.1 and 5.2. It can be noted that y and Fr^{-1} tend to decrease with decreases in ratio S/L, as expected. Fr^{-1} is plotted against S/L in each case in Fig. 5.1 and 5.2. From the intercepts and slopes of the straight lines, values of m and x_N for different extractants can be obtained. Another important inference is the limiting value of extraction as S/L tends to zero in each case. This value, given by $(x_o - x_N)/x_o$, is the maximum fractional extraction possible for a particular extractant. The limiting value should be as close to one as possible. Table 5.3 summarizes the conclusions drawn from Fig. 5.1 and 5.2.

Table 5.1: Equilibrium Runs on the Tailings of First Shipment

x_0 = 394.378 pCi/g Time of Contact: 2 to 3 hrs

	Extractant*	$\frac{S}{L}$ Ratio	y pCi/g	$\frac{1}{Fr} = \frac{Sx_0}{Ly}$	Remark
1.	Water	0.1667	1.94	33.88	Fig. 5.1a
		0.0833	1.12	29.33	
		0.0666	1.11	23.68	
2.	Water (60°C)	0.1667	1.46	45.03	Fig. 5.1a
		0.1111	1.84	23.81	
		0.0666	1.21	21.73	
3.	1 M $CaCl_2$	0.2270	16.87	5.307	Fig. 5.1b
		0.1323	12.49	4.177	
		0.0926	9.73	3.753	
		0.0772	10.45	2.913	
		0.0579	7.57	3.016	
4.	0.3 M EDTA [Ethylene-diamine tetra-acetic acid (sodium salt)]	0.2358	39.22	2.371	Fig. 5.1b
		0.1886	34.25	2.172	
		0.1572	40.92	1.515	
		0.1179	25.64	1.813	
		0.0858	18.77	1.803	
5.	8.2% DTPA [Diethylene-triamine-pentasodium salt]	0.1887	25.09	2.966	Fig. 5.1b
		0.1179	21.50	2.163	
		0.0858	18.69	1.810	
		0.0674	13.79	1.927	

* At room temperature unless otherwise mentioned. The solutions are prepared in distilled water.

Table 5.2: Equilibrium Runs on the Tailings of Second Shipment

x_0 = 768.410 pCi/g Time of Contact: 2 to 3 hrs

	Extractant*	$\frac{S}{L}$ Ratio	y pCi/g	$\frac{1}{Fr} = \frac{Sx_0}{Ly}$	Remarks
1.	6.65% DTPA	0.1916	89.33	1.648	Fig. 5.2
		0.1197	63.75	1.443	
		0.0871	44.88	1.491	
		0.0684	35.82	1.467	
2.	40.5% HNO_3	0.1639	87.44	1.440	Fig. 5.2
		0.1025	59.44	1.313	
		0.0745	42.02	1.362	
		0.0585	31.63	1.421	
3.	9.2% HCl	0.1923	21.04	7.023	Trend in y is
		0.1202	65.02	1.420	not as expected,
		0.0874	103.09	0.651	$\frac{1}{Fr}$ being less than
		0.0687	97.31	0.542	1.0 is not possible.

* At room temperature. The solutions are prepared in distilled water.

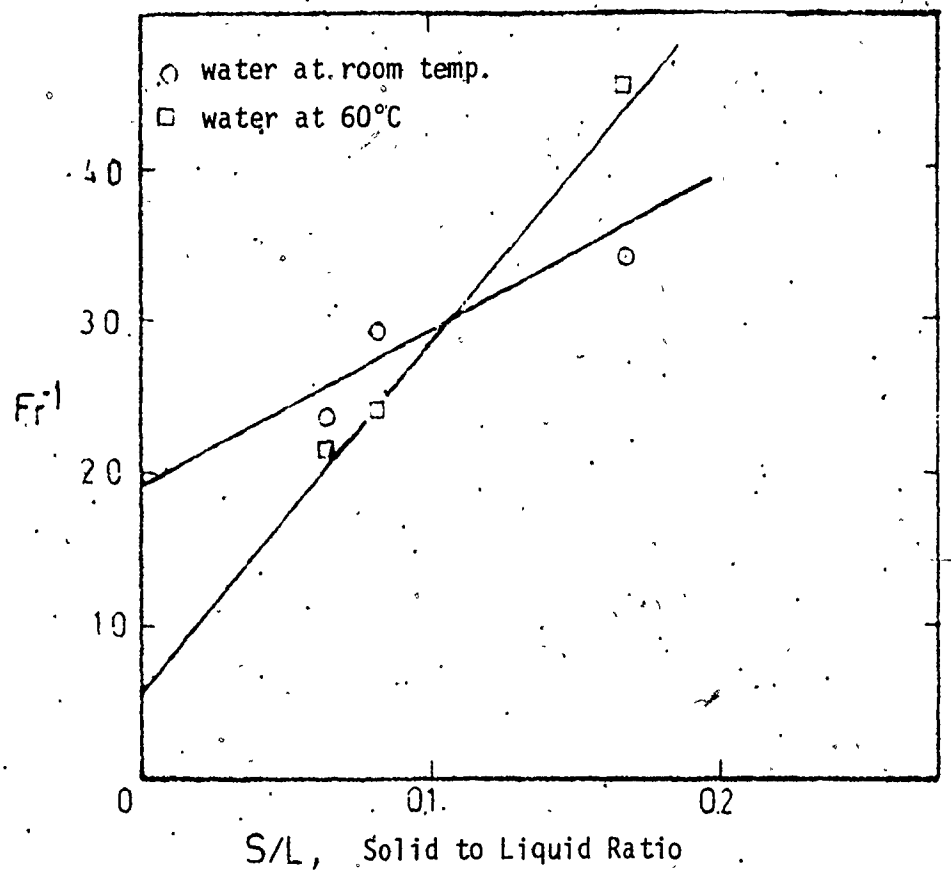

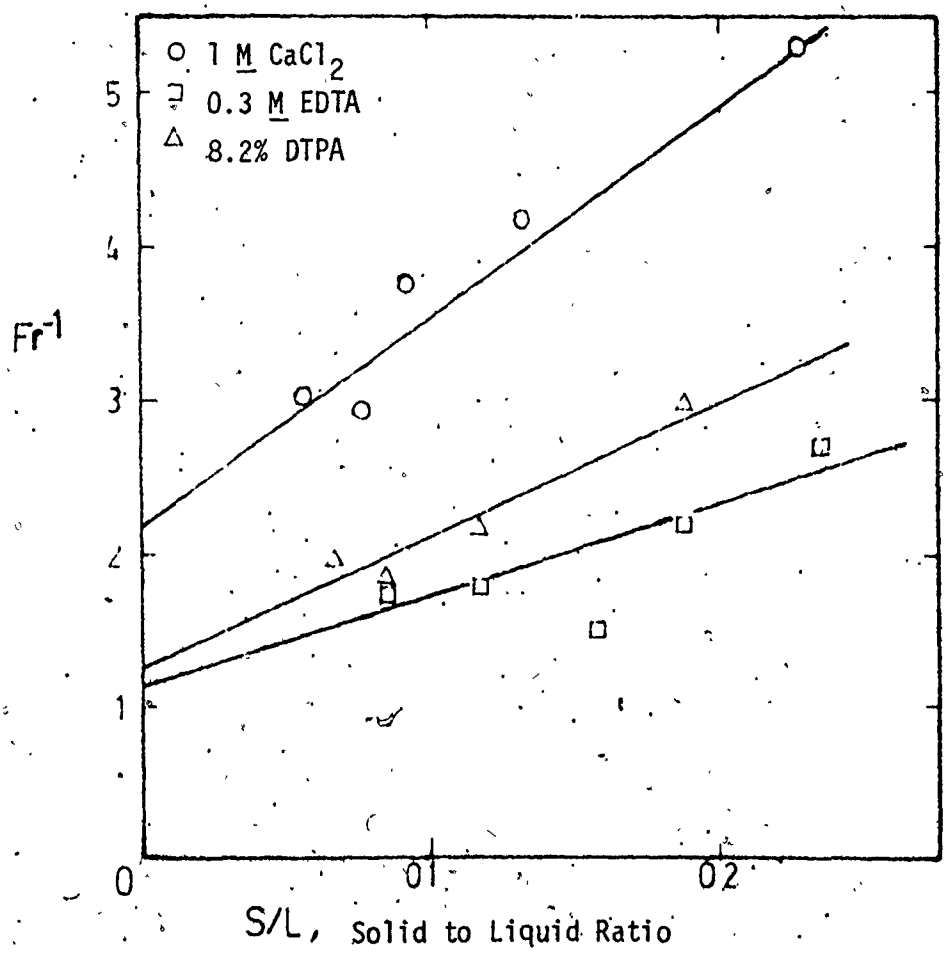

Figures 5.1(a) and (b) Effect of S/L on Extraction of Radium from Tailings of the First Shipment (Average Particle Size 144 μ)

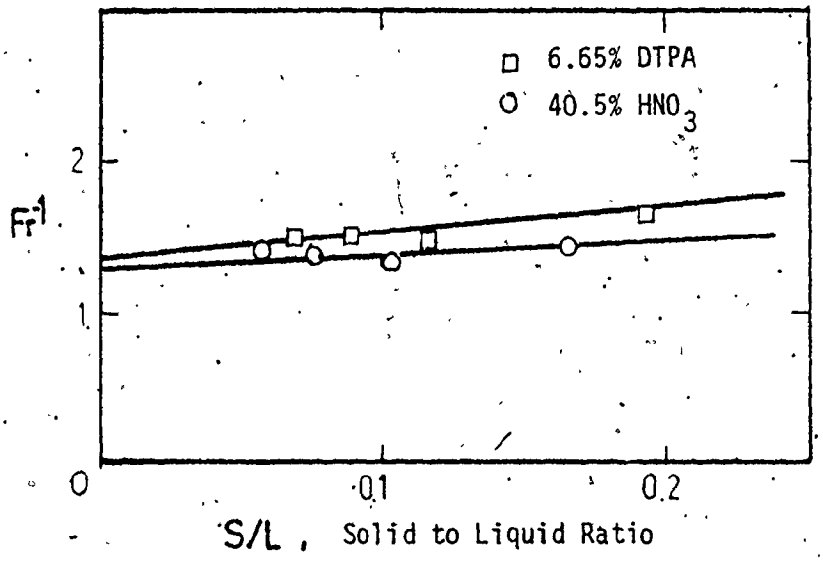

Figure 5.2 Effect of S/L on Extraction of Radium from Tailings of the Second Shipment (Average Particle Size 128 μ)

Table 5.3: Calculations from Figs. 5.1 and 5.2

Shipment	Extractant	Intercept $\frac{x_0}{x_0 - x_N}$	Slope $\frac{x_0}{m(x_0 - x_N)}$	x_N pCi/g	m	Limiting Fractional Extraction, Fr*
First	Water (Room Temp.)	19.0	102.77	373.6	0.18	0.053
First	Water (60°C)	5.5	234.78	322.7	0.02	0.182
First	1 M $CaCl_2$	2.15	13.81	210.9	0.15	0.465
First	8.2% DTPA	1.25	8.84	78.9	0.14	0.800
First	0.3 M EDTA	1.15	6.10	51.4	0.19	0.870
Second	6.65% DTPA	1.35	1.73	199.2	0.78	0.741
Second	40.5% HNO_3	1.30	0.89	177.3	1.46	0.769

The average particle size of the tailings in the first shipment was larger than that of the second shipment, the latter being considerably higher in the radium content. This perhaps explains the slight difference in the performance of DTPA (of slightly different concentrations) on the two types of tailings.

Some interesting inferences can be made from the results and graphs presented so far in this section. Hot water (60°C) is better than water at room temperature up to a certain S/L ratio close to 0.1, beyond which the latter is better (Fig. 5.1a). However, in both the cases, water extracts extremely low amounts of radium. 1 M $CaCl_2$ is intermediate whereas HNO_3, EDTA and DTPA show good prospects for removal of radium from the tailings. In general, the flatter the straight line on Fr^{-1} vs. S/L plot the better the extractant.

5.3 . KINETIC RUNS

Several leaching experiments were carried out with fixed S/L ratio but varying time of contact with several extractants. The extractants were distilled water, 1 M $CaCl_2$, 0.3 M EDTA, 6.65% DTPA and 40.5% HNO_3. For each extractant, six batches with time of contact ranging from a few minutes to several hours (varied in geometric progression) were leached out. The purpose of these experiments was to investigate the effect of varying time of contact on the extraction of radium.

Tables 5.4.a through 5.4.g present the results from these experiments. From the measured values of y and the calculated values of x (Eqn 3), "accountability" defined by equation 10 is calculated in each case. In view of the extremely small quantities of radium involved in

Tables 5.4 a-g: Effect of Time of Contact on Radium Extraction

Table 5.4.a: Water at Room Temp., $\frac{S}{L} = 0.1111$, $x_0 = 374.378$ pCi/g

Expt.	Time (hrs)	x' pCi/g	y pCi/g	x pCi/g	Accountability %	$Fr = \frac{Ly}{Sx_0}$
1	0.25	365.73	0.13	461.51	117.32	0.0030
2	0.5	326.31	1.01	414.14	107.32	0.0230
3	1	355.94	0.46	451.21	115.46	0.0105
4	2	348.43	0.75	449.95	115.80	0.0171
5	4	284.06	∿ 0.0	340.87	86.43	∿ 0.0
6	18	254.98	∿ 0.73	317.81	82.25	0.0167

Table 5.4.b: 1 M $CaCl_2$, $\frac{S}{L} = 0.2273$, $x_0 = 394.378$ pCi/g

Expt.	Time (hrs)	x' pCi/g	y pCi/g	x pCi/g	Accountability %	$Fr = \frac{Ly}{Sx_0}$
1	0.5	221.24	11.07	271.68	81.24	0.1235
2	1	208.05	17.12	263.80	85.99	0.1910
3	2	120.91	15.88	138.22	52.76	0.1771
4	4	185.69	16.87	229.24	76.95	0.1882
5	8	142.52	17.75	187.94	67.45	0.1980
6	17	197.47	14.57	283.43	88.12	0.1625

Table 5.4.c: 0.3 M EDTA, $\frac{S}{L}$ = 0.2358, x_0 = 394.378 pCi/g

Expt.	Time (hrs)	x' pCi/g	y pCi/g	x pCi/g	Accountability %	Fr = $\frac{Ly}{Sx_0}$
1	0.5	124.98	40.29	143.27	79.65	0.4332
2	1	169.91	36.95	202.35	91.04	0.3973
3	2.25	148.15	39.22	170.81	85.48	0.4217
4	4	143.37	35.03	165.90	79.73	0.3766
5	8	144.88	38.73	168.66	84.41	0.4165
6	16	160.28	33.66	184.59	83.00	0.3619

Table 5.4.d: 0.3 M EDTA, $\frac{S}{L}$ = 0.1886, x_0 = 394.378 pCi/g

Expt.	Time (hrs)	x' pCi/g	y pCi/g	x pCi/g	Accountability %	Fr = $\frac{Ly}{Sx_0}$
1	0.5	145.35	34.86	151.53	85.29	0.4618
2	1	138.49	32.92	181.56	90.30	0.4426
3	2	131.29	34.25	155.94	85.59	0.4605
4	4	112.01	27.70	156.52	76.93	0.3724
5	8	177.11	32.32	215.33	98.05	0.4345
6	16	148.26	25.33	164.98	75.89	0.3405

Table 5.4.e: 0.3 M EDTA, $\frac{S}{L} = 0.1179$, $x_0 = 394.37$ pCi/g

Expt.	Time (hrs)	x' pCi/g	y pCi/g	x pCi/g	Accountability %	$Fr = \frac{Ly}{Sx_0}$
1	0.5	106.23	19.12	122.95	72.30	0.4112
2	1	116.55	26.57	139.94	92.63	0.5714
3	2	137.41	25.64	171.61	98.66	0.5514
4	4	132.24	25.36	160.67	95.28	0.5454
5	8	69.73	29.58	75.28	82.60	0.6350
6	16	81.33	26.90	87.60	80.06	0.5785

Table 5.4.f: 6.65% DTPA, $\frac{S}{L} = 0.1197$, $x_0 = 768.41$ pCi/g

Expt.	Time (hrs)	x' pCi/g	y pCi/g	x pCi/g	Accountability %	$Fr = \frac{Ly}{Sx_0}$
1	0.25	104.61	68.59	111.74	89.11	0.7571
2	0.50	81.66	70.66	83.79	87.73	0.7799
3	1	109.75	68.78	117.45	90.06	0.7592
4	2	91.05	63.75	98.20	82.09	0.7037
5	4	95.83	68.61	100.08	87.62	0.7573
6	8	70.44	63.47	71.83	78.35	0.7006

Table 5.4.g: 40.5% HNO_3, $\frac{S}{L}$ = 0.1025, x_0 = 768.41 pCi/g

Expt.	Time (hrs)	x' pCi/g	y pCi/g	x pCi/g	Accountability %	$Fr = \frac{Ly}{Sx_0}$
1	0.25	146.00	52.02	176.82	89.06	0.6605
2	0.83	138.74	47.95	161.92	69.25	0.4818
3	1.5	82.84	55.72	85.55	81.89	0.7074
4	2	98.35	59.98	103.18	89.58	0.7615
5	2.5	87.34	57.32	93.76	84.98	0.7278
6	10	47.65	52.85	46.95	73.21	0.6710

this work and the uncertainties in measurement of x', accountabilities between 80% to 120% were considered satisfactory.* Once again, the fractional removal of radium was based on the y values.

It is not clear whether the extraction of radium is only due to simple physical dissolution or also due to a chemical reaction between radium (which is perhaps in the form of $RaSO_4$ in the tailings) and the extractant. The results from the kinetic runs were expected to throw some light on the kinetics of the chemical reaction if that is what actually occurs. Based on intuition, it was expected that y (and hence Fr) would increase with the time of contact until the equilibrium is established.

The results do not show any such trend. The y values remain fairly constant with time and the scatter is perhaps due to experimental errors. The results do make it quite clear that the equilibrium dissolution of radium (by whatever mechanism) is quite rapid. It takes less than half an hour for most of the extractants to leach a substantial amount of radium, and merely increasing time of contact up to 18 hours does not improve the removal of radium. The term "equilibrium" is used here in the sense that no significant change is seen over a time in the order of 10 hours; it does not imply that changes may not occur over a much longer period.

The results from the Tables 5.4.a through 5.4.g are graphically presented in Fig. 5.3.a through 5.3.g, respectively. It can be noted that the y values are reasonably close to each other whereas the x values have more scatter in each case. This confirms the previous contention about uncertainties in the measurement of x'.

---

* In Table 5.4.a, some values of x even exceed x_0, clearly indicating the possible errors and uncertainties in counting (Also see section 5.1.2).

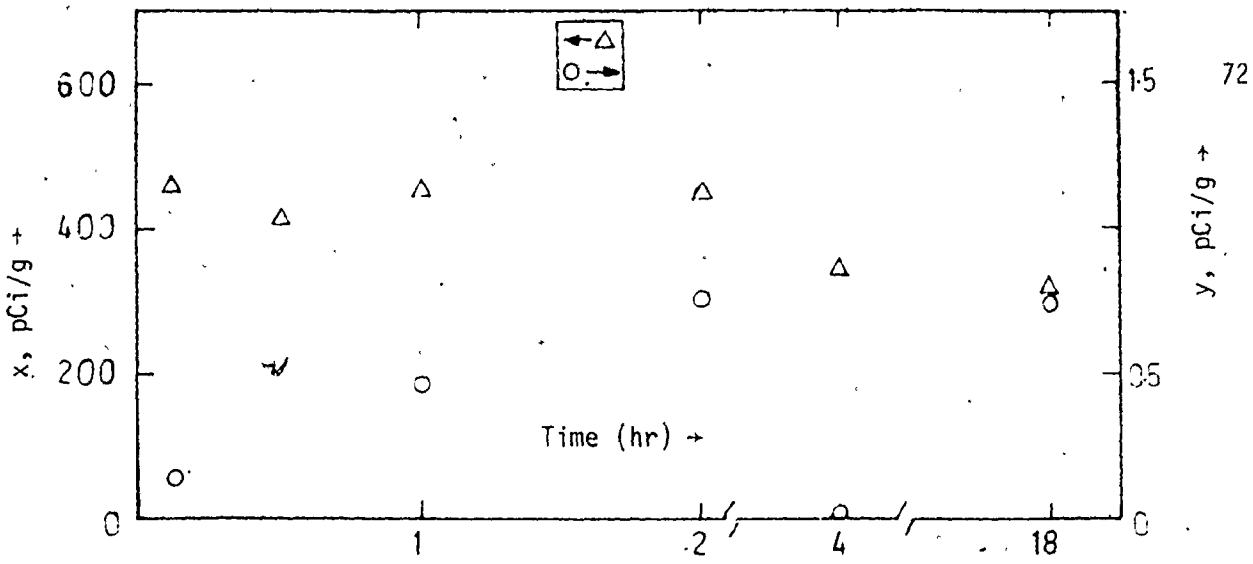

Figure 5.3a Water at Room Temp., Table 5.4.a

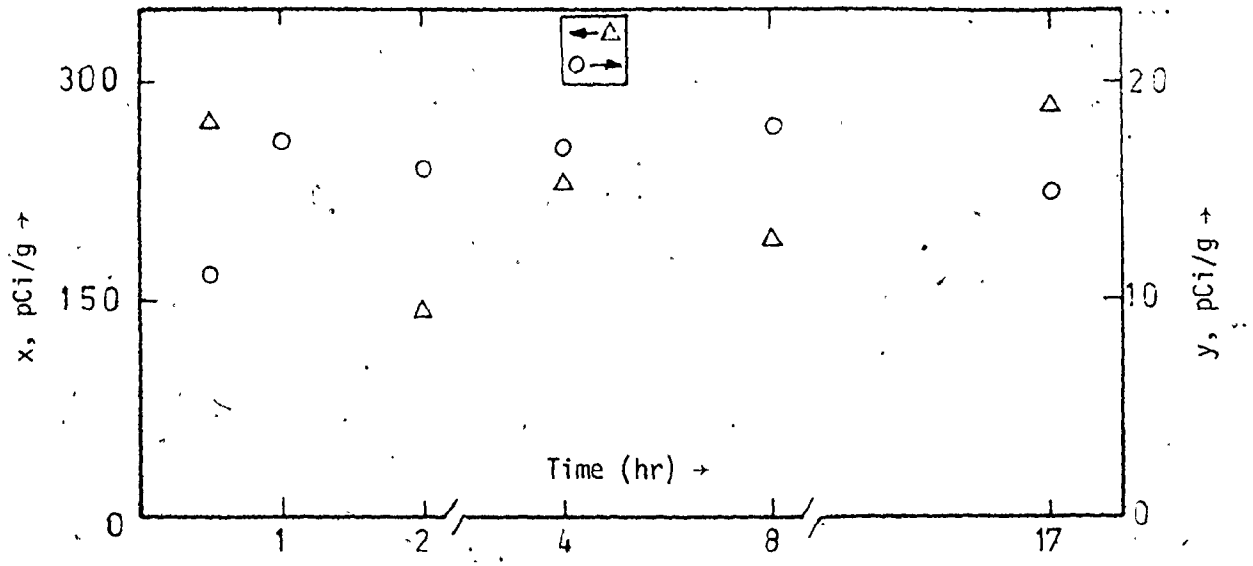

Figure 5.3b 1 M $CaCl_2$, Table 5.4.b

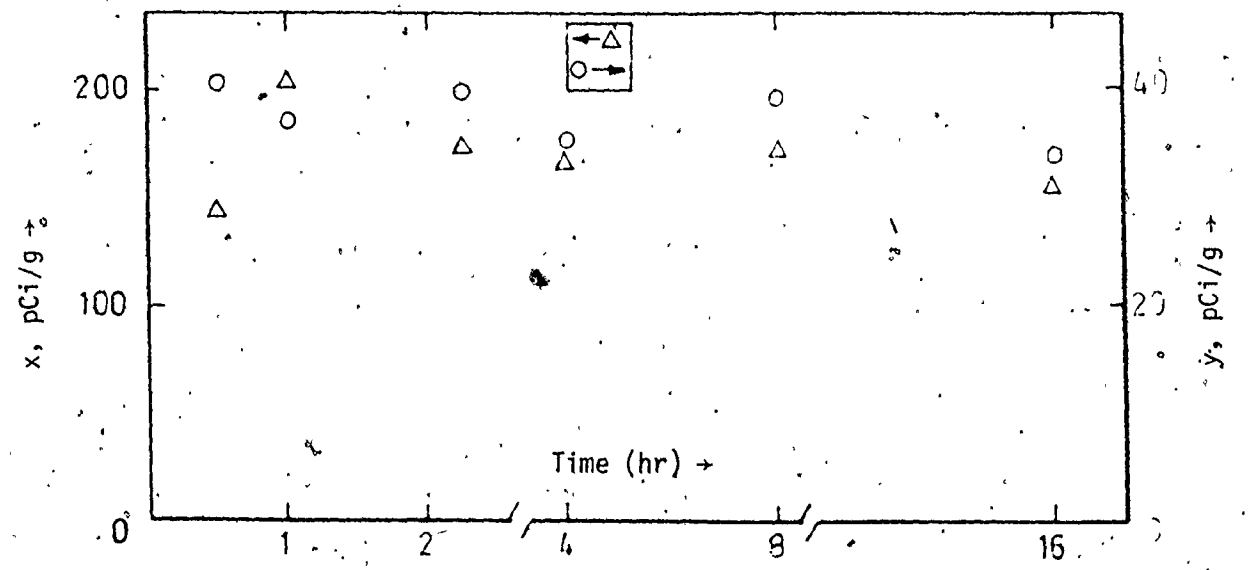

F[illegible] 0.3 M

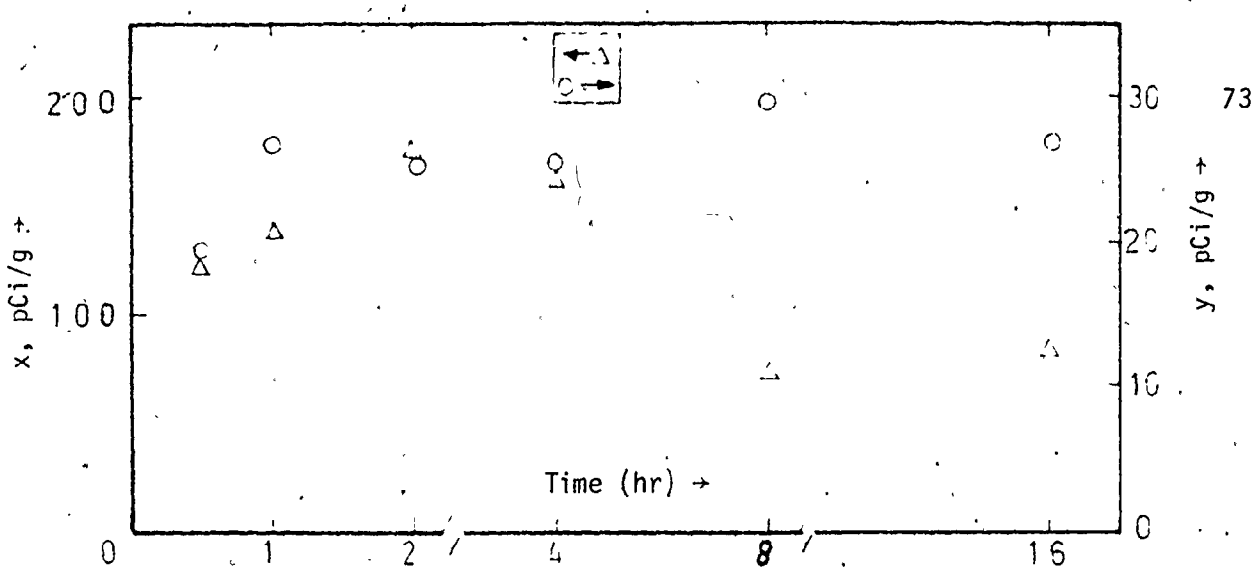

Figure 5.3d 0.3 M EDTA, Table 5.4.d

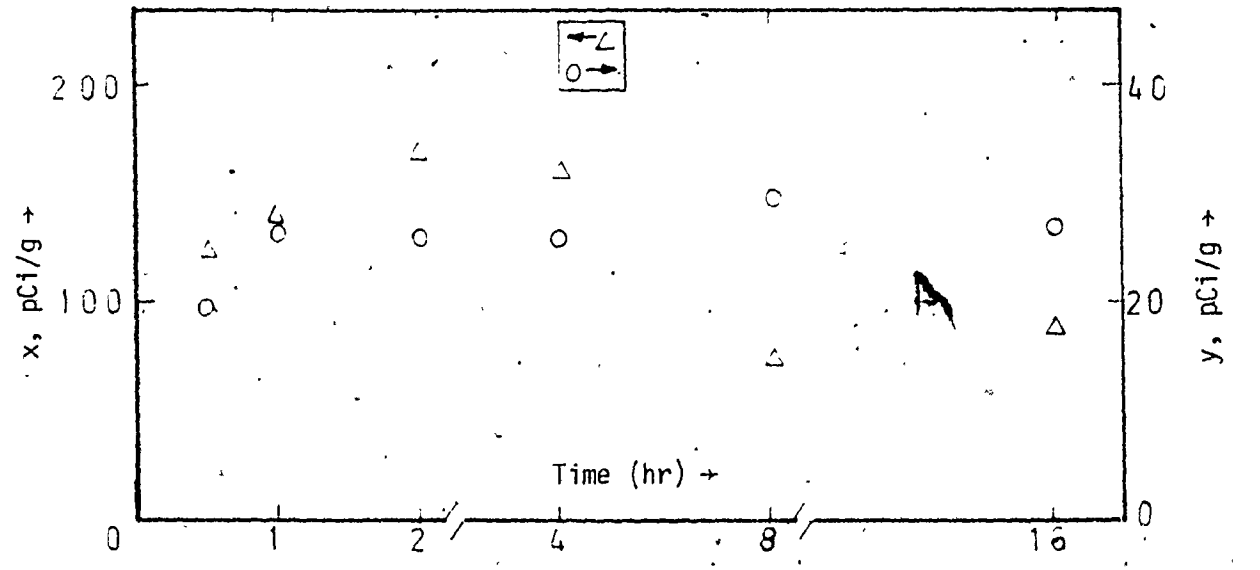

Figure 5.4e 0.3 M EDTA, Table 5.4.e

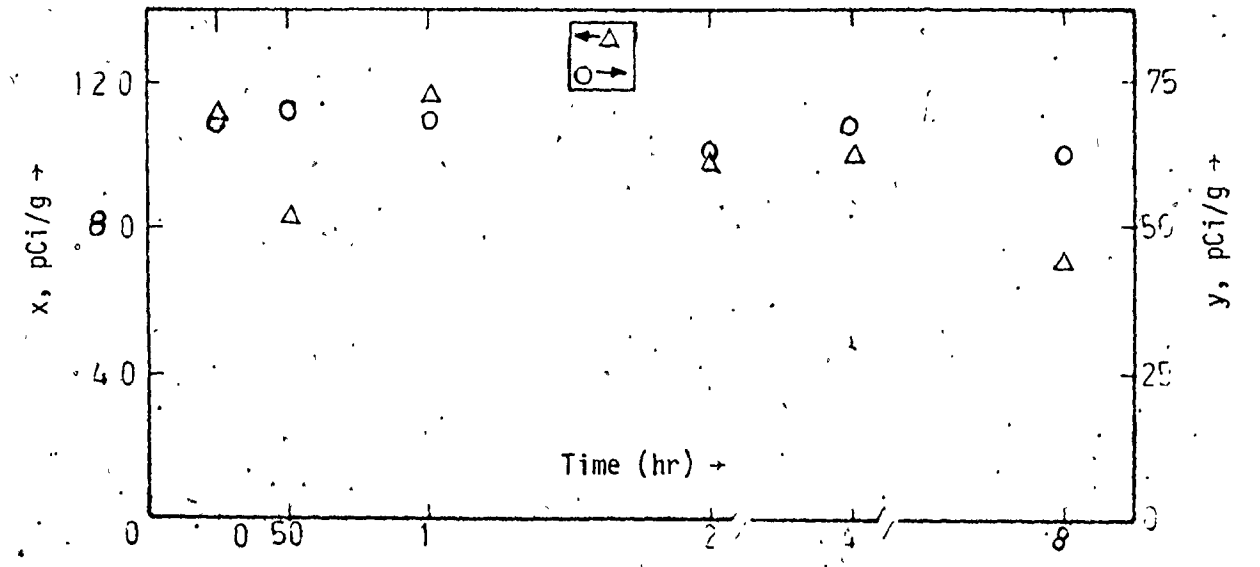

re DTPA. Tab 5.4.f

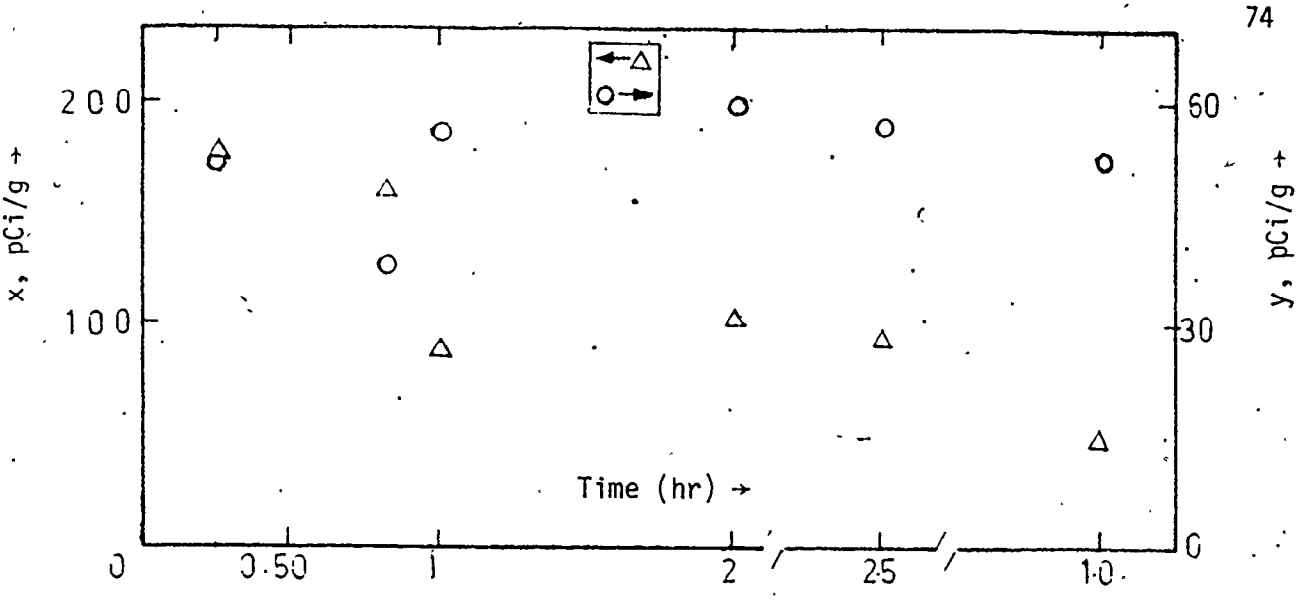

Figure 5.3g - 40.5% HNO_3, Table 5.4.g

Figure 5.3 (a) through (g) Ra^{226} Concentration in Solid and Liquid Phase Plotted Against Time of Contact for Kinetic Runs with Various Extractants

5.4 ADDITIONAL EXPERIMENTS

The performance of 1 M $CaCl_2$ was reasonably good as an extractant of radium (Table 5.3). This extractant becomes particularly interesting as it is cheap. It was, therefore, decided to investigate $CaCl_2$ leaching in more detail. First, it was decided to find out the effect of varying $CaCl_2$ concentration. Second, a series of successive batch contactings were done. Due to time limitation, only one set of experiments was performed in each case.

5.4.1 Effect of concentration: Different solutions of $CaCl_2$ in water up to a concentration 2 M were used as extractants. Leaching experiments were performed in each case with constant S/L ratio. The time of contact was two hours in each experiment. The data from the distilled water extractant (Section 5.2) were used to extrapolate the results for zero concentration of $CaCl_2$.

Table 5.5 gives the results. The results are graphically plotted in Fig. 5.4.a and 5.4.b. Interestingly, the removal of radium increases up to about 1 M $CaCl_2$ beyond which there is no improvement. It is likely that other extractants also have such an optimum concentration. Such information is quite useful in any process design for the chemical removal of radium from the tailings.

5.4.2 Multiple Batch Contacting: Fig. 5.5 details the exact way in which a three-stage crosscurrent batch contacting was carried out. The S/L ratio was held constant in each stage. As expected, the y values decrease as the stage number increases. The fractional removal of radium is calculated

Table 5.5: Effect of Concentration of $CaCl_2$ Solution on the Removal of Radium from the Tailings

($\frac{S}{L}$ = 0.0772, x_0 = 374.378 pCi/g)

Conc. of $CaCl_2$	y pCi/g	$Fr = \frac{Ly}{Sx_0}$	$\frac{1}{Fr}$
0.0* M	1.12	0.034	29.33
0.25 M	7.16	0.235	4.25
1.0 M	10.45	0.343	2.91
2.0 M	10.59	0.347	2.87

* From the closest $\frac{S}{L}$ data on distilled water at room temperature.

Table 5.6: Results from the Multiple Batch Contacting

[Extractant 1 M $CaCl_2$, x_0 = 394.378 pCi/g, $\frac{S}{L}$ = 0.0772 (constant)]

Stage No. n	y_n pCi/g	Σy_n pCi/g	$Fr_n = \frac{L(\Sigma y_n)}{Sx_0}$
1	8.93	8.93	0.2934
2	2.14	10.77	0.3638
3	1.26	12.03	0.3953

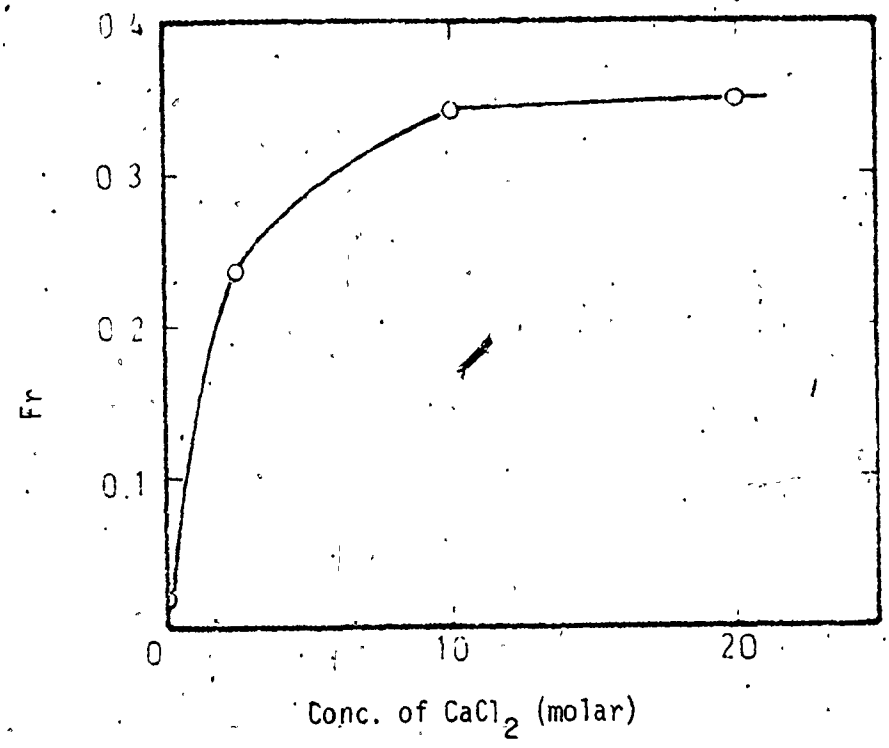

(a)

Figure 5.4 Effect of conc. of $CaCl_2$ on the Extraction of Radium (the trend as conc. approaches zero is interpreted from equilibrium data on distilled water)

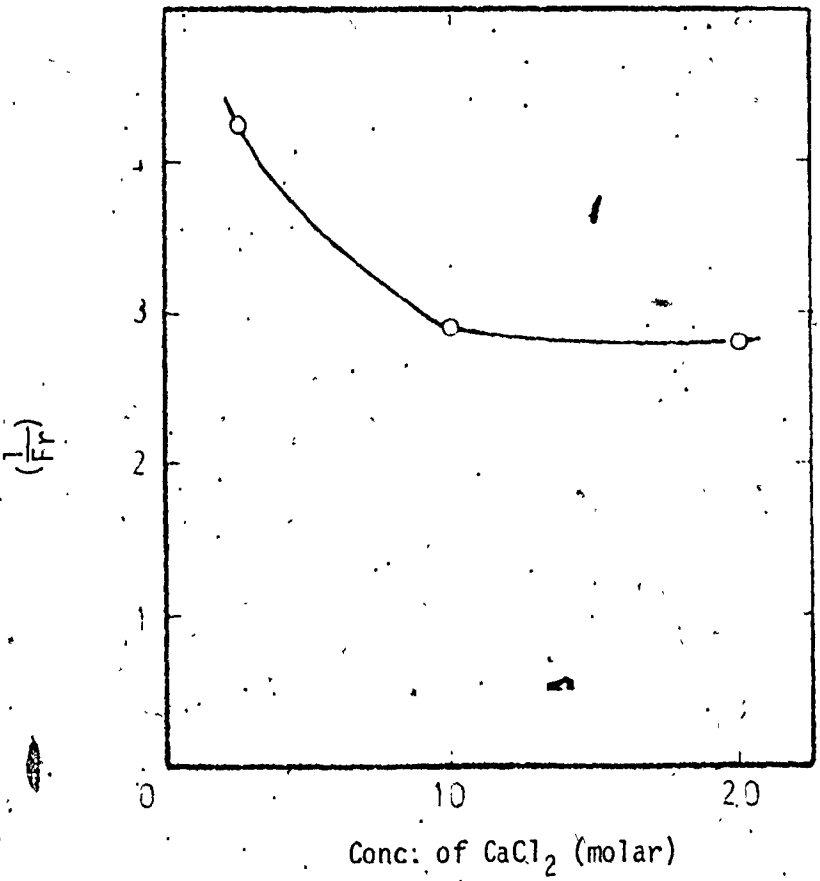

(b)

Figure 5.5: Scheme of Three Stage Contacting (Time of Contact in Each Stage 2.5 hrs)

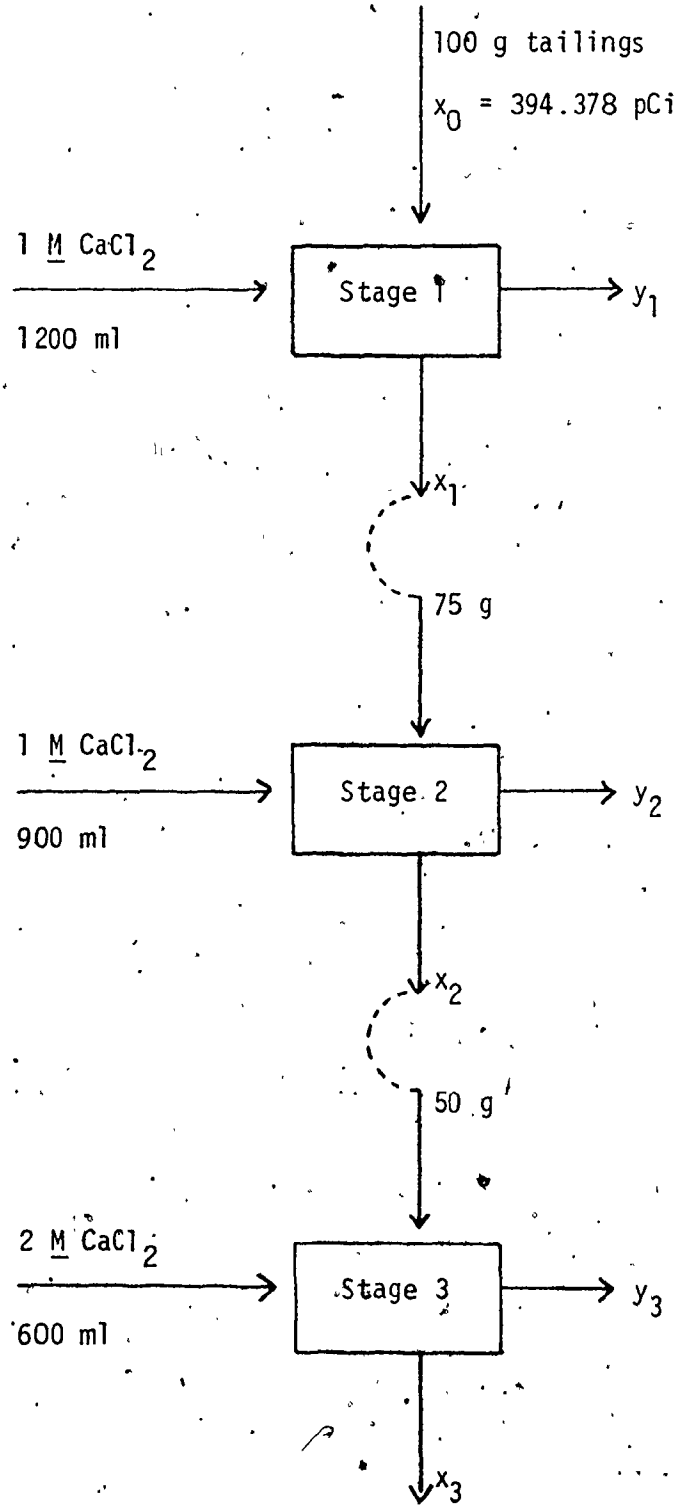

in a cumulative fashion from stage to stage. The results are reported in Table 5.6. Since y decreases at a decreasing rate from stage to stage, Fr_n would increase as stage number increases but at a decreasing rate.

CHAPTER 6

CONCLUSIONS AND RECOMMENDATIONS

The work done so far should be considered a reasonable stopping point in the overall problem of radium extraction from mill tailings. To develop an extraction scheme on the large scale, much still remains to be done. Obviously, extensive studies of process design, economic feasibility and pilot plant runs are necessary before implementing any scheme of this type. The present work was confined to some fundamental studies on a bench scale. In this last chapter, Conclusions from the present work and recommendation for future work are given.

6.1 CONCLUSIONS

The following conclusions are based on this work:

(1) The average accountability of radium in this work was 86.12% with a standard deviation of ± 12.44%, which indicates that the gamma counting technique is reasonably accurate.

(2) For the tailings from both the shipments, the major weight fraction was below 75 microns particle size. In general, the radium content in pCi/g increased with decreasing particle size. The radium to weight ratio varied between 0.7 and 1.4. The largest size fraction of particles showed a relatively high radium concentration but there is photographic evidence that these consisted of agglomerates.

(3) All the extractants studied show a linear equilibrium relation between concentrations in the liquid and the solid phases. There is a constant fraction of radium which is retained in the tailings, irrespective of solid/liquid ratio employed. The constant depends on the extractant used.

(4) All the extractants studied leach out a certain amount of radium within a few minutes. Increasing time of contact up to 18 hours does not improve on this initial extraction of radium.

(5) There may be an optimum concentration for every extractant beyond which any increase in the concentration does not increase the amount of radium extracted. (This was found for $CaCl_2$ solutions.)

(6) Multiple batch cross current contacting improves the performance of an extractant. The fraction of radium removed increases at a decreasing rate as the number of stages are increased.

6.2 RECOMMENDATIONS FOR FUTURE WORK

There are several lines of further experimental investigation which could be taken up on the basis of present work. Some of them are briefly discussed in this section.

(1) Most of the extractants studied showed fast kinetics (c.f. Section 5.3). It is, however, not clear whether a chemical reaction between radium (in whatever form it is present in the tailings) and the extractant plays any role in the removal of radium from the tailings. To study this aspect, it would be necessary to modify the experimental technique so that the time of contact could be kept very short (i.e., from a few seconds to a few minutes).

(2) The difference in leachability of radium from the tailings of two different shipments indicates that particle size is an important variable in this study. Leaching experiments with various sieve fractions should be carried out to find more about the dependence on particle size.

(3) Almost all the leaching experiments were carried out at room temperature for this work. It would be interesting to investigate the effect of temperature on the extraction of radium. Also as it has been found out in the present work, that in the case of $CaCl_2$ the removal of radium depends on the concentration of $CaCl_2$ solution (c.f. Section 5.4.1), experiments should be carried out with a number of other extractants.

(4) Multiple contacting is very versatile in making maximum use of the extractability of an extractant. Based on the laboratory procedure developed in the present work, multiple batch contacting experiments (c.f. Section 5.4.2) can be easily extended for a number of other extractants.

REFERENCES

1. Williams, R.M., "Uranium", (1978 Annual Review and Forcast), Canadian Mining Journal, No. 2, p. 153 (1978).
2. Katz, J.J. and Robinowitch, E., "The Chemistry of Uranium", National Nuclear Energy Series, Div VIII, Vol. 5, Part 1 (1951).
3. Galkin, N.P., et al., "The Technology of Treatment of Uranium Concentrates", International Series of Monograph on Nuclear Energy, Div IX, Vol. 1 (1963).
4. Cember, H., "Introduction to Health Physics", Pergamon Press (1976).
5. Benedict, M. and Pigford, T.H., "Nuclear Chemical Engineering", McGraw Hill Book Company (1957).
6. Hurst, F.J., "Safety in Uranium Mining and Milling", Nuclear Safety 4, No. 1, p. 68 (1962).
7. Elliot, D.M. and Weawer, L.E. (Editors), "Education and Research in Nuclear Fuel Cycle", University of Oklahoma Press (1972).
8. Gitlus, G.H., "Uranium", Butterworths, London (1963). [In Metallurgy of Rarer Metals - 8.]
9. Moffet, D., "Uranium Waste Researchers Consider Alternate Means of Tailing Disposal", Canadian Mining Journal, No. 1, 48 (1977).
10. Gordon, J.F. (Consulting Editor), "The Nuclear Fuel Cycle: A Survey of the Public Health, Environment, and National Security Effects of Nuclear Power", Union of Concerned Scientist (1975), The M.I.T. Press Environment Study Series.
11. WIN-112, Winchester Laboratory: Topical Report, Jan. 1960, USAEC Document.

12. Seeley, F.G., "Problems in the Separation of Radium from Uranium Ore Tailings", Hydrometallurgy, 2, p. 249 (1977).

13. Shearer, S., "The Leachability of Ra^{226} from Uranium Mill Waste Solids and River Sediments", Ph.D. Thesis, University of Wisconsin (1962).

14. Kolthoff, I.M. and Elving, P.J. (Editors), "Treatise on Analytical Chemistry", Part II, Vol. 4, Section A, p. 219 (1966).

15. Fink, R.M., "Biological Studies with Polonium, Radium and Plutonium", National Nuclear Energy Series, Div VI, Vol. 3, McGraw Hill Book Company (1950).

16. Goldsmith, W.A., "Radiological Aspects of Inactive Uranium Milling Sites: An Overview", Nuclear Safety 17, No. 6 (1976).

17. Borrowman, S.R. and Brooks, P.T., "Radium Removal from Uranium Ores and Mill Tailings", Report of Investigation 8099, Bureau of Mines, U.S. Department of the Interior (1975).

18. Franklin, J.C., et al., "Polymeric Sealants May Provide Effective Barriers to Radon Gas in Uranium Mines", Engineering and Mining Journal 176, 116 (1965).

19. Skeaff, J.M., "Distribution of Ra^{226} in Uranium Tailings", Report MRP/MSL 76-137(J), Mineral Research Program, Canmet (1976).

20. Ryan, R.K. and Alfredson, P.G., "Laboratory Studies of the Treatment of Liquid Waste Streams from Uranium Milling Operations", Proc. Australas. Inst. Min. Metall., No. 253 (1975).

21. Arnold, W.D. and Course, D.J., "Radium Removal from Uranium Mill Effluents with Inorganic Ion Exchangers", I & EC Process Design and Development 4, No. 3, p. 333 (1965).

2 2

OF/DE

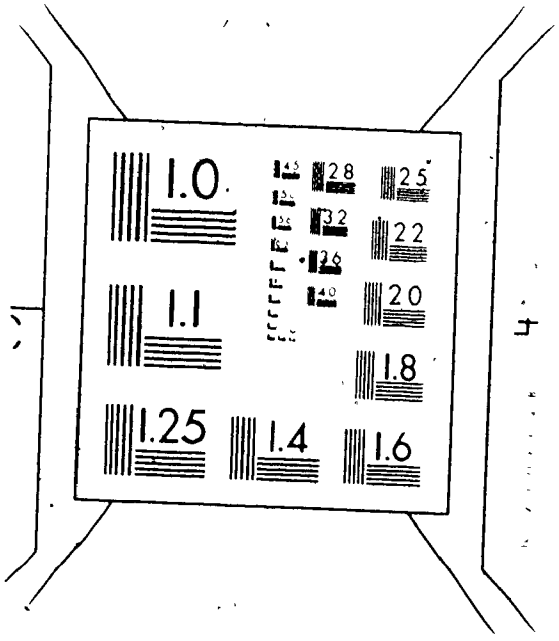

22. WIN-116, Winchester Laboratory: Quarterly Report, Jan.-March, 1960, USAEC Document.

23. Birks, F.T., UKAEA Report AERE C/R 2774 (1959) (Referred to in (14) above).

24. Brandao, F.A. et al., "The Employment of Liquid Emulsion for the Estimation of Uranium from Radioactive Minerals", Proc. of Intl. Conf. on Peaceful uses of Atomic Energy 8, p. 274, Geneva (1955).

25. Mann, W.B., "A Radiation Balance for the Microcalorimetric Comparison of Four National Radium Standards", Journal of Research of National Bureau of Standards, Vol. 53, No. 5, p. 277 (1954).

26. Rushing , D.R. et al., "The Anlaysis of Effluents and Environmental Samples from Uranium Mills and of Biological Samples for Radium, Polonium and Uranium", in Radiological Health and Safety in Mining and Milling of Nuclear Materials, Vol. II, IAEA, Vienna, 1964, p. 187.

27. Darrall, K.G. et al., "An Emanation Method for Determining Radium Using Liquid Scintillation Counting", Analyst, 98, p. 610 (1973).

28. Goldin, A.S., "Determination of Dissolved Radium", Analytical Chemistry, 33, p. 406 (1961).

29. Zimmerman, J.B. and Armstrong, V.C., "The Determination of Ra^{226} in Uranium Ores and Mill Products by Alpha Energy Spectrometry", Report 76-11, Mineral Research Program, Canmet (1975).

APPENDIX A: Specifications of Counting Set-up

APPENDIX B: Ingrowth Period and Secular Equilibrium

APPENDIX C: Self-Shielding in Samples

APPENDIX D: Effect of Unleached Th^{230}

APPENDIX E: Statistical Error Analysis

APPENDIX A

SPECIFICATIONS OF COUNTING SET-UP

Specifications of the detector, associated electronics and shielding used in the counting set-up:

Component	Remarks	Setting
1. Ge(Li) Detector	Canberra Industries (Model 7228), Crystal circular Cylindrical drifted co-axially, dia. 36 mm, length 25 mm.	---
2. Power Supply	Tennelec, TC 908	1000 V
3. Preamplifier	Nuclear Data Inc.	---
4. Linear Amplifier	Tennelec, TC 202	Coarse Grain: 100 Fine Grain: 6.15 Restorer: out Shaping: unipolar Polarity: Inverted Output: DC couple
5. SCA	Tennelec, TC 440	LLD: 0.26 ULD: 6.56 Mode E_2-E_1
6. Scalar	Canberra Industry (Model 1473)	---

Component	Remarks	Setting
7. Shielding	Cylindrical Lead Shielding (c.f. Fig. 3.1.a) Thickness = 3.4 cm Outer Dia. = 15.3 cm Height = 15.0 cm Thickness of cover = 2.5 cm	---

APPENDIX B

INGROWTH PERIOD AND SECULAR EQUILIBRIUM

It will be shown here that after an adequate ingrowth period (about 40 days), the count rate of 609 KeV gamma ray of Bi^{214} is a measure of radium content of a particular sample. In other words, a state of secular equilibrium is established between radium and its daughters in this period and hence the amount of each radionuclide is proportional to its half-life.

The part of Uranium Series which is of interest here is:

$$Ra^{226} \xrightarrow[1622\ y]{} Rn^{222} \xrightarrow[3.82\ d]{} Po^{218} \xrightarrow[3.05\ min]{} (Cont'd)$$

$$\longrightarrow Pb^{214} \xrightarrow[26.8\ min]{} Bi^{214} \xrightarrow[19.7\ min]{} \ldots$$

Let N_j be a number of atoms of j^{th} radionuclide at any time t, beginning with j = 1 from Ra^{226}. In these notations, the decay series is

$$N_1 \xrightarrow[\lambda_1]{} N_2 \xrightarrow[\lambda_2]{} N_3 \xrightarrow[\lambda_3]{} \ldots \longrightarrow Ni \xrightarrow[\lambda_i]{} \ldots \longrightarrow N_7 \xrightarrow[\lambda_7]{}$$

Here λ_j are the decay coefficients which are related to corresponding half-lives:

$$\lambda_j = \frac{\ell n 2}{\text{Half-life of } j^{th} \text{ radionuclide}}$$

and N_5 is Bi^{214} whose gamma peak is being counted.

It will be assumed that:

$$\text{At } t = 0 \qquad N_1 = N_1^0$$

$$N_i = 0 \quad \text{for } i = 2 \ldots$$

This assumption is reasonable because most of the Rn^{222} quickly emanates out of tailings. Even if some free radon is trapped in the void volume of the solid samples or is dissolved in the liquid samples, it will decay to a negligible amount in 40 days, i.e., more than ten times its half-life. The same is true for all other radionuclides from i = 3 .. 7, as they are still shorter-lived compared to Rn^{222}.

An atom balance on the i^{th} radionuclide at anytime t is

$$\frac{dNi}{dt} = \lambda_{i-1}N_{i-1} - \lambda_i N_i \qquad \text{for } i = 2 \ldots \tag{1a}$$

and for Ra^{226},

$$N_1 = N_1^0 e^{-\lambda_1 t} \tag{1b}$$

Equations of the above type for N_1 to N_7 can be solved successively for given initial conditions. One gets*

$$N_i = \lambda_1\lambda_2 \ldots \lambda_{i-1}N_1^0 \sum_{j=1}^{i} \frac{e^{-\lambda_j t}}{\prod_{k\neq j}(\lambda_k - \lambda_j)} \tag{2}$$

For i = 5

---

* Benedict, M. and Pigford, T.H., "Nuclear Chemical Engineering", McGraw-Hill Book Company (1957).

$$N_5 = \lambda_1\lambda_2\lambda_3\lambda_4 N_1^0 \left[\frac{e^{-\lambda_1 t}}{(\lambda_2 - \lambda_1)(\lambda_3 - \lambda_1)(\lambda_4 - \lambda_1)(\lambda_5 - \lambda_1)}\right. \quad (3)$$

$$\left. + \frac{e^{-\lambda_2 t}}{(\lambda_1 - \lambda_2)(\lambda_3 - \lambda_2)(\lambda_4 - \lambda_2)(\lambda_5 - \lambda_2)} + \cdots + \frac{e^{-\lambda_5 t}}{(\lambda_1 - \lambda_5)(\lambda_2 - \lambda_5)(\lambda_3 - \lambda_5)(\lambda_4 - \lambda_5)}\right]$$

Due to the very long half-life of Ra^{226} (1622 y) and short half-lives of all other radionuclides (the longest of them being 3.82 days for Rn^{222}), the following approximations can be made in eqn. (3):

(a) for t = 40 days or more, $e^{-\lambda_2 t}$, $e^{-\lambda_3 t}$, etc. are all very small compared to $e^{-\lambda_1 t}$ which is very close to unity, so except for the first term, the rest of the six terms in the square bracket can be discarded as being negligibly small;

(b) for the denominator of the first term in the square bracket, subtraction of λ_1 can be discarded as being negligible compared to λ_2, λ_3, etc. in each of the brackets.

In this way, eqn. (3) becomes

$$N_5 \simeq \lambda_1\lambda_2\lambda_3\lambda_4 \frac{e^{-\lambda_1 t}}{\lambda_2\lambda_3\lambda_4\lambda_5}$$

Using (1b), this becomes

$$N_5 \simeq \frac{\lambda_1}{\lambda_5} N_1$$

or

$$N_1 \propto (t_{1/2})_1$$

and

$$N_5 \propto (t_{1/2})_5$$

It shows that secular equilibrium exists.

APPENDIX C

SELF-SHIELDING IN SAMPLES

Self-shielding effects are only of secondary importance for this work as long as they are similar for every sample and standard. Since solid and liquid standards were separately prepared and every effort was made to maintain constant geometry, it is expected that self-shielding will be the same in each case, and calculated values of radium concentration will not be effected.

However, it is worthwhile to discuss self-shielding in solid and liquid samples to determine whether or not this has any major effect on measured activity as compared to total activity.

Fig. C-1 shows a typical situation. A sample of density ρ, thickness t and surface area S is placed near the detector. Let I_m be measured activity (i.e., with self-shielding), I_t be the total activity (i.e., when there is no self-shielding effect) and A be the specific activity.

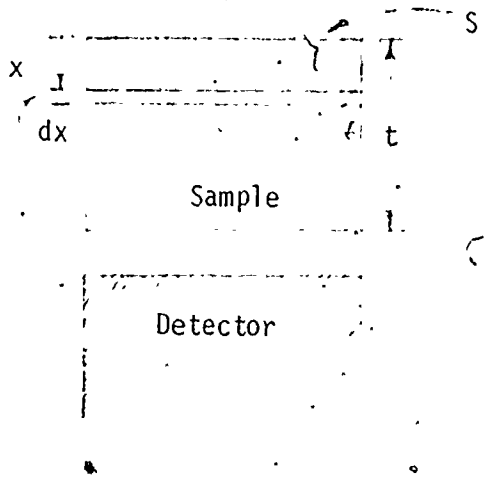

Figure C-1

For a thin element of thickness dx, one can write

$$dI_m = \frac{1}{2} A(Sdx)\cdot\rho e^{-\mu_\ell (t-x)} \qquad (1)$$

Here μ_ℓ is linear coefficient of self-attenuation. The factor $\frac{1}{2}$ is there because the detector is receiving signals from only one face of the element.

Integrating (1) from x = 0 to t,

$$I_m = \frac{ASp}{2\mu_\ell}(1 - e^{-\mu_\ell t}) \qquad (2)$$

For no self-shielding, however,

$$I_t = \frac{1}{2}A(Sp)t \qquad (3)$$

Comparing (2) and (3) and defining a self-shielding factor f, we can write,

$$I_m = I_t * f$$

where

$$f = \frac{1 - e^{-\mu_\ell t}}{\mu_\ell t}$$

f should be as close to unity as possible to minimize self-shielding effects. The value of μ_ℓ depends on gamma-ray energy also. For the present case, interpolated values*,† for 609 KeV gamma energy for SiO_2 and water

---

* Siegbahn, K., "Alpha, Beta and Gamma Spectroscopy", Vol. 1, North-Holland Publishing Co. (1965).

† Cember, H., "Introduction to Health Physics", Pergamon Press (1976).

were used for solid and liquid samples, respectively. Table C-1 gives the calculated value of f from μ_ℓ values in the literature.

Table C-1 Self-Shielding Factor for Solid and Liquid Samples

Samples	t,cm	μ_ℓ,cm^{-1}	f
Solid	5	0.182	0.656
Liquid	6	0.091	0.770

It should be noted that this derivation is valid for large distances between the sample and detector.

APPENDIX D

EFFECT OF Th^{230} IN THE TAILINGS FROM WHICH Ra^{226} HAS BEEN REMOVED

Th^{230} is the precursor of Ra^{226} in the Uranium Series. When tailings are treated to remove Ra^{226} only, Th^{230} is left behind. Obviously, this Th^{230} will slowly build-up Ra^{226} in the "treated" tailings. In this appendix effect of the residual Th^{230} on subsequent growth of Ra^{226} is discussed. Finally an explanation is given to justify the particular attention given to removal of Ra^{226}.

The initial portion of the Uranium Series is rewritten below:

$$U^{238} \xrightarrow[4.51 \times 10^9 \text{ y}]{} Th^{234} \xrightarrow[24.1 \text{ d}]{} {}^{m}Pa^{234} \xrightarrow[1.12 \text{ min}]{} {}^{g}Pa^{234} \xrightarrow[6.66 \text{ h}]{} \text{(Cont'd)}$$

$$\longrightarrow U^{234} \xrightarrow[2.48 \times 10^5 \text{ y}]{} Th^{230} \xrightarrow[8.0 \times 10^4 \text{ y}]{} \text{(Cont'd)}$$

$$\longrightarrow Ra^{226} \xrightarrow[1622 \text{ y}]{}$$

The purpose here is to derive a smple expression for amount of Ra^{226} in terms of time elapsed after the tailings are treated. The following simplifying assumpgions will be made:

(a) Uranium Series was initially in secular equilibrium in the ore. Of course, the equilibrium is disrupted by dil H_2SO_4 leaching;

(b) U^{238} and U^{234} are both totally removed from the ore in the leaching process for uranium extraction. (This is justified because isotopes

behave in the same fashion chemically.);

(c) Th^{234}, $^{m}Pa^{234}$, $^{g}Pa^{234}$ are short-lived and their concentrations become negligible before tailings are treated for Ra^{226} removal;

(d) The treatment removes all the Ra^{226} and no Th^{230} from the tailings.

The last assumption is disputable. In practice, 100% removal of Ra^{226} may not be possible. Also, Th^{230} may have some leachability in the extractant used to remove Ra^{226}. However, for approximate calculations of subsequent growth of Ra^{226}, this assumption is useful.

After the treatment of the tailings, with above assumption we have the decay process beginning with Th^{230} as follows:

$$Th^{230} \xrightarrow[8.0 \times 10^4 \text{ y}]{} Ra^{226} \xrightarrow[1622 \text{ y}]{} Rn^{222} \longrightarrow \ \ldots$$

or, in the usual notation,

$$N_1 \xrightarrow{\lambda_1} N_2 \xrightarrow{\lambda_2} N_3 \longrightarrow \ \ldots$$

With initial condition

$$\text{At } t = 0 \qquad N_1 = N_1^0$$
$$N_i = 0 \qquad i = 2, 3, \ldots$$

Here, N_1^0 must be same as initial Th^{230} content of the ore as it is assumed that Th^{230} is not removed either in ore processing or in treatment of the tailings.

The governing eqns. for N_1 and N_2 are

$$\frac{dN_1}{dt} = -\lambda_1 N_1 \qquad (1)$$

$$\frac{dN_2}{dt} = \lambda_1 N_1 - \lambda_2 N_2 \qquad (2)$$

Solving for N_2

$$N_2 = \frac{\lambda_1}{\lambda_2 - \lambda_1} N_1^0 (e^{-\lambda_1 t} - e^{-\lambda_2 t}) \qquad (3)$$

For maximum radium concentration at $t = t_m$

$$\left.\frac{dN_2}{dt}\right|_{t = t_m} = 0$$

or

$$t_m = \frac{1}{\lambda_2 - \lambda_1} \ell n \frac{\lambda_2}{\lambda_1} \qquad (4)$$

Substituting actual values for λ_1 and λ_2

$$t_m = 9313.14 \text{ y} \approx 10{,}000 \text{ y}$$

Substituting t_m in eqn. (3)

$$\left.\frac{N_2}{N_1^0}\right|_{max} = 0.018704$$

Eqn. (3) is plotted on a semi-logrithm graph in Fig. D-1.

In the untreated tailings, Ra^{226} and Th^{230} amounts will be proportional to their respective half-lives. Thus, for untreated tailings,

$$\frac{N_2}{N_1^0} = 0.020282$$

The foregoing discussion suggests that if most of Ra^{226} is removed

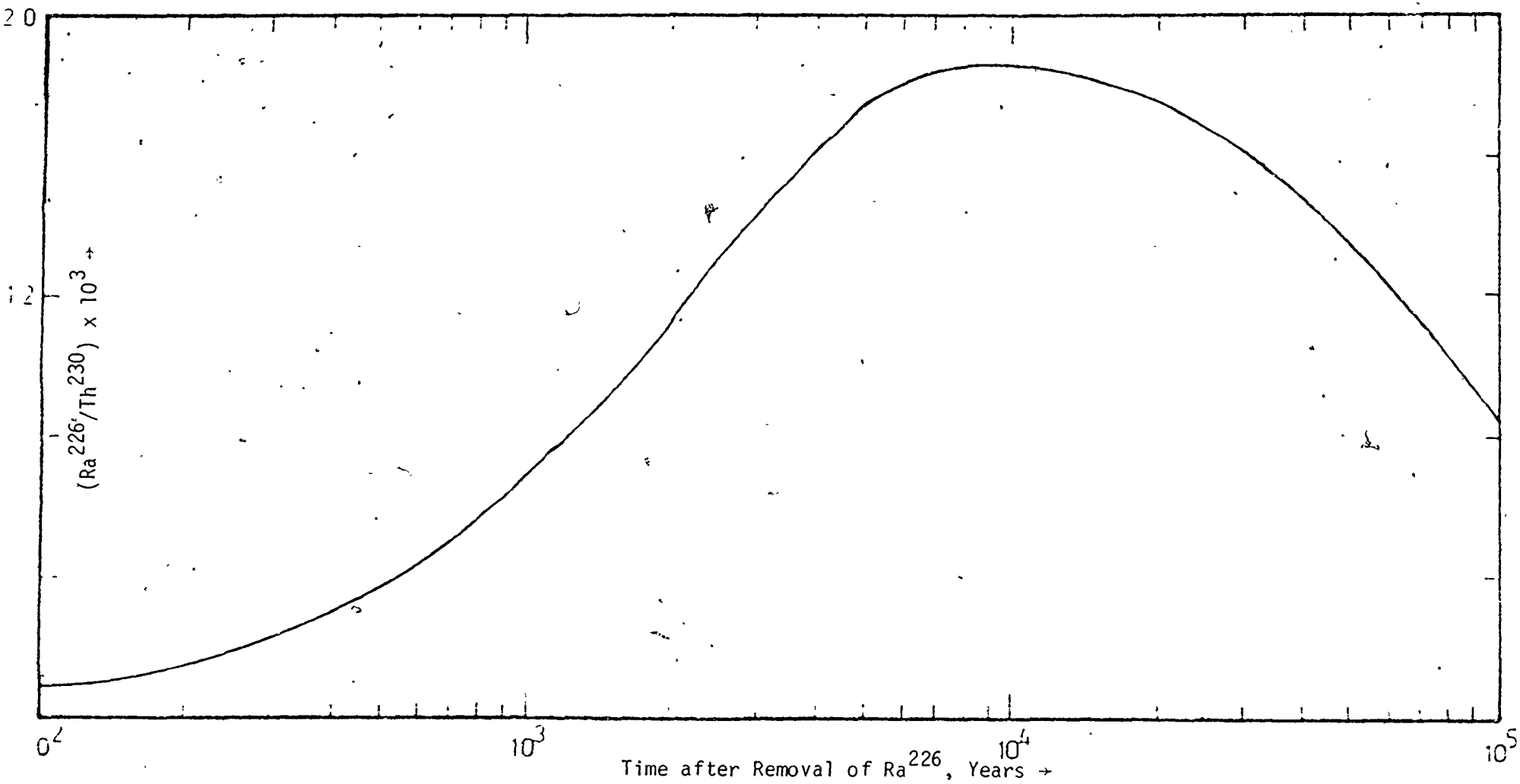

Figure D-1 Effect of Unleach Th^{230}

from the tailings, its subsequent growth due to Th^{230} decay is extremely slow. The Ra^{226} amount will reach a maximum in about 10,000 years. Even at this maximum, Ra^{226}/Th^{230} ratio is about 8% lower than that in untreated tailings. These along with the fact that Ra^{226} is far more toxic than Th^{230} justifies the particular attention being paid to the removal of Ra^{226}.

APPENDIX E

STATISTICAL ERROR ANALYSIS

Statistical errors introduced in counting typical liquid and wet solid samples are discussed in this Appendix. The observed counts include the background counts as well as the counts associated with the sample. The background was counted several times for 12-18 hours using solid and liquid blank samples (c.f. Section 4.1). If the standard deviation is used as an index of precision, the percentage error in the count rate for counting n counts is $100/\sqrt{n}$ (c.f. Section 3.6).

If the total count rate is $r_t \pm a$ and the background count rate is $r_b \pm b$, then the true count rate r will be given by

$$r = (r_t - r_b) \pm \sqrt{a^2 + b^2} \qquad (1)$$

Table E-1 gives the data on five of the several background countings done in this work.

Table E-1: Background Counting

Counting Time (hrs)	18.75	14.16	16.00	13.33	11.75
Counts	3500	2748	3100	2507	2227
Background Count rate, r_b counts/hr	186.66	193.97	193.75	188.02	189.53
% error in r_b	1.69	1.90	1.80	1.99	2.12

From Table E-1, the average value of r_b rounded off to the nearest whole number is 190 counts/hr with an average error of 1.9%. Thus, r_b

can be expressed as 190 ± 3.6.

Table E-2 gives the data on total count rate, r_t, and calculated error bars in the true count rate r using equation (1) for typical solid and liquid samples. Counting data for two solid and two liquid samples were arbitrarily taken from the Kinetic Runs. However, these data in Table E-2 and the estimated errors are representative of this current work. It should be noted that Tables 5.4 (a through g) do not give detailed counting data.

Table E-2: Total Counts of Typical Samples

Counting Time (min)	75	43	75	59
Counts	1295	1035	1649	1165
Total count rate, r_t counts/hr	1036	1444.2	1319.2	1184.7
% error in r_t	2.78	3.11	2.46	2.92
r_t expressed as $r_t \pm b$	1036 ± 28.8	1444 ± 44.9	1319 ± 32.4	1185 ± 34.6
True count rate r, counts/hr	846 ± 29	1254 ± 45	1129 ± 32	995 ± 34.8

Thus, typically there is an error of ± 35 counts/hr for the samples. From the slopes of the calibration curves this implies the error bars are approximately ± 130 pCi for wet solid samples and ± 240 pCi for liquid samples is introduced. These errors can also be expressed as an equivalent concentration of radium in pCi/g because wet solid and

liquid samples typically weighed 30 g and 110 g, respectively. Thus, in pCi/g the errors are as follows:

Wet Solid Samples $\pm$ 4.33 pCi/g

Liquid Samples $\pm$ 2.18 pCi/g

In this analysis, only the statistical errors are considered significant; other experimental errors are not identified specifically.